

Dear Prof. Erwin Zehe:

I am very sorry that I missed your comments in the last round. This is partly because I am not familiar with the HESS's system, which is distinguished from that of the other journals. Please believe that as a senior researcher, I really understand the values of your work and will never intentionally disregard the comments of yours and the reviewers'.

As you suggested, I revised the manuscript again. Major revisions include: 1) I added Figure 1 and Appendix E to exhibit how the LI method works and its validity in a straightforward way; 2) As you suggested, I added a supplement that details the calculation steps of LI method; 3) I requested the Editage (www.editage.cn), a division of Cactus Communications, helped me with the language editing.

Sorry again about my failure last round.

Best regards

Mingguo Zheng
2020-3-1

Response to Editor

Editor Decision: Reconsider after major revisions (further review by editor and referees) (16 Jan 2020) by Erwin Zehe

Comments to the Author:

Dear Prof Mingguo Zheng.

I had a close look at your manuscript, the two reviews and your corresponding responses. In line with reviewer 2 I see that the proposed approach to assess and discriminate model sensitivities to climate and catchment characteristics is more general than what you call the total differential. The latter corresponds to the derivative of a multivariate function if and only if the variables are orthogonal. This must not be the case for hydrological state variables as you correctly stated.

Many thanks for your careful examination of the manuscript. But I felt that you seem to misunderstand the method we present in the manuscript. The method is distinct from the existing ones in that it is mathematically precise. For this reason, I revised the title as "A mathematically precise method to partition climate and catchment effects on runoff". I do not think that the method is more general than the existing ones. Moreover, it equally requires that the independent variables are orthogonal.

Acceptance of a new method for publication of requires however, a) a convincing demonstration of its relevance and b) a clear and broadly understandable explanation of the underlying math, particularly in comparison to other existing methods. The present manuscript should be considerably improved respect to both issues. This requires major revisions, which should address the reviewers' recommendations.

a) I intentionally emphasized the research significance many times in the manuscript, such as lines 34-41, 75-88, 326-337, and 348-354. I will certainly add more if the reviewer could be more specific.

b) Figures 4-7 all aims to compare with other existing methods. In the revised version, I added Figure 1 in comparison to the methods in a straightforward way and a supplement that details the calculation steps of LI method.

Moreover I recommend you should consider the following issues during the revision process:

- As I am not sure, whether all partial derivatives of R are correct, I recommend that you provide a supplement which details the important steps to facilitate the evaluation/understanding of the math.

This is a good advice. As suggested, I added a supplement that details the calculation step using one of the catchments as an example.

- How strong is the actual dependence of precipitation and potential evaporation? This is of key importance to evaluate, whether the new methods needs to be used or not.

I added the correlation analyses at lines 321-325 and addressed the issue of the interdependence of the climate and catchment variables.

It was found that although annual P and E_0 showed significant correlation, the mean annual P and E_0 showed little correlation (see the figure below).

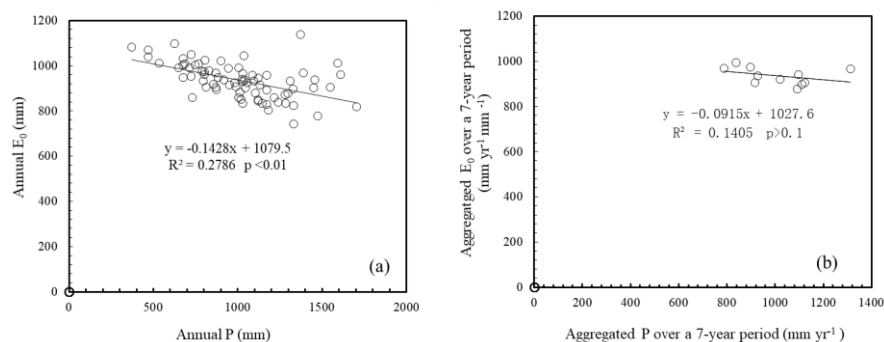


Figure R1 There is good correlation between annual P and E_0 (a) for the Adjungbilly CK , but the correlation tapers off when aggregated over a 7-year period (b).

- With all the respect I have for the Budyko framework, for me n is like a fitting factor. Of course we expect that offsets from the Budyko curves are explainable with catchment characteristics, but this should much be more precise- is it landuse, total soil storage volume, field capacity and retention properties or what are we talking about. The latter can be investigated in a straightforward manner with a conceptual hydrological model. The current way how this issue is addressed is way too unspecific.

I re-read the references of the selected catchments. For all of them, the change in catchment properties mainly referred to the vegetation cover or land use change. I have added the statement in Lines 238-239.

I adopted a “tuned” n value that can get exact agreement between the calculated E and that actually encountered, so that the offsets you mentioned are very small for all established Budyko models.

The object of the manuscript is to present a new method using the Budyko model as an example, and did not intend to do something about the Budyko model itself. I am sorry I did not do anything more.

- I agree that changes have different impacts on non-linear dynamics when they occur during different systems state and thus on different points in time. However, I doubt that the Budyko framework is suitable for working this out, because it refers to the steady state water balance. A dynamic system catchment under change will develop from old to a new steady state behavior. Why should this new steady state functioning depend on the time where the change occurred?

At a given state, the state functioning depends on the sensitivities at the state. In Figure 1, for example, we would concern $f'(x)$ as $\Delta z_x = f'(x)dx$ at point A, and $f'(x+\Delta x)$ as $\Delta z_x = f'(x+\Delta x)dx$ at point C. Similarly, we would concern the sensitivities at all points along the curve AC if the change from the state A to C occurs. That's why the LI method concerns all points along AC.

I am not sure I have understood the comments. Using the Budyko framework to partition the effects of human activities and climate change is a common practice in the hydrology community. The steady state water balance is indeed prerequisite to the use of the Budyko framework requires. When a catchment evolves from old to a new steady state, however, the catchment is dynamic but not steady.

- Last but not least you should make sure that you manuscript is in line with the common guidelines for equations and variables published on the HESS webpage.

I have read the guidelines and revised the equations and units.

Response to Reviewer 1

Many thanks for your insightful comments and careful examination of the manuscript. I have studied your comments carefully and tried our best to revise the manuscript. My responses are given as follows. Attached please find the revised version. Thank you and best regards.

1. [This manuscript describes mathematical research. The application is to a classical hydrological problem but the results are about comparing (theoretical) calculated quantities. In more detail, the formulation of the problem addressed in described in detail on pages 2-3 (lines 77-89). The basic idea is that the standard first order expansion for a total differential does not adequately consider the order of the differentiation. A new proposal is made that enables the first order expansion to be used. In short I did not understand the proposed formulation of the problem.]

This manuscript developed a new method. I think that it is quite needed to compare the method with the existing ones.

This research was motivated by the lack of a mathematically precise method to partition the combined effect of several drivers (Line 40-41). In lines 77-89, we further stated that the problem does not get solved even given a precise hydrology model.

2. [To my mind this is classical calculus and it may be better to get a professional mathematician to evaluate the work. My own evaluation is that I could not see the underlying point of the formulation. On my understanding (and remembering that I am not a professional mathematician) we use a first order expansion to get the total differential, and each of the individual differentials are considered to be infinitesimal in which it does not matter about the order. If we want more detail then we make a second order expansion, e.g., using the example from the text, i.e., $R=f(x, y)$, we have for the relevant second order term a differential like; $\partial^2 R/(\partial x \partial y)$ to more fully account for the missing part. Such rigour is rarely used in Hydrological (or science) practice since we usually have finite differences (rather than differentials) and the necessary accuracy is usually only 10% or so.]

Yang et al (2014) have shown that the first order expansion has caused an error of the climate impact on runoff ranging from 0 to 20 mm (or -118 to 174%) over China. Although the error is sometimes trivial, anyway, a precise method is always desirable.

Reference

Yang, H., D. Yang, and Q. Hu: An error analysis of the Budyko hypothesis for assessing the contribution of climate change to runoff. *Water Resources Research*, 50, 9620–9629, 2014.

Response to Reviewer 2

Many thanks for your insightful comments and careful examination of the manuscript. I have studied your comments carefully and tried our best to revise the manuscript. My responses are given as follows. Attached please find the revised version. Thank you and best regards.

1. [The paper describes a mathematical method to attribute a discrete change in runoff to changes in climate and catchment characteristics. The method is directly applicable to common data and yields quite similar results when compared to existing methods. However, it remains open which of these methods is more accurate because there is no data to verify.]

I acknowledge that the empirical evidence is indeed lacking. However, our method is mathematically precise but the others are not. The mathematical

reasoning is as powerful as the empirical evidence.

In addition, although the test data is usually unavailable, it is easily obtained in the one-dimension case. Figure 1 clearly demonstrated that the LI method yields precise results but the others does not in the case of a univariate function.

2. [Still, there are two interesting and valuable aspects of the manuscript: a) The role of the evolution over time b) Reconciling the existing methods and their assumptions on this evolution]

They are indeed the key points of the LI method and the manuscript.

3. [To consider the path of changes is an important aspect and, as the author illustrates, may thus alter the resultant sensitivity to a change. This is important, since this may allow to better assess the vulnerability of a given catchment to global change. The problem is, that there is usually not sufficient data to constrain the evolution of disturbances.]

I acknowledged that this is indeed the limit of the LI method. I have added a paragraph to discuss the high data requirement associated with the LI method. See line 298-302 for details.

4. [The author uses subperiods of 7 years, where at least the meteorological data provides some constraints. However, the use of shorter periods comes at the cost of potential changes in the catchment water storage, which can then be misinterpreted as changes in catchment characteristics. Figure 6 shows that the temporal variation of the catchment property sensitivity is largest. This might actually be caused by water storage changes, rather than actual changes in the catchment properties. This aspect is not sufficiently discussed in the manuscript.]

I have added a paragraph to addressed the aggregated time period associated with the Budyko model. See Lines 303-320 for details.

5. [Although I like that the existing methods are discussed in detail, I strongly recommend that the author better visualizes these methods. An attempt is done in Figure 1, but this must be extended and linked to the other methods.]

As suggested, I have added Figures 1 and 2.

6. [Recommendation: Major Revisions. The relevance/significance of the paper must be better highlighted. This requires major changes throughout.]

I intentionally emphasized the research significance many times in the manuscript, such as lines 34-41, 75-88, 326-337, and 348-354.

I understand the importance to clearly show the research significance to readers. I have considered this suggestion seriously. Could you be more specific about why and how?

7. [Further comments: Overall, the notation should be more consistent (for example

indices)and streamlined]

I have checked the notation throughout the manuscript.

8. [I think that some parts of the paper can be cut. Figure 2b is trivial and can be removed]

A major conclusion of the manuscript is that the decomposition method is a special case of the LI method. Figure 2b lends direct support to the conclusion so that it is not trivial. I am sorry I do not cut it.

9. [It would be better to describe the decomposition method in a conceptual Figure, similar to Fig.1.]

I have added Figure 2 as you suggested.

10. [The catchments with the largest changes in n have a reference period of only 3 years. This is quite short for a reference period.]

I am sorry that I indeed directly used the data given in Zhou et al (2016). Many thanks for your careful examination .

I do not remove the catchment (NO.10 in Table 1) from the manuscript considering the reasons below: 1) the catchment has a high aridity index of 1.5. In dry areas, the carryover of soil water storage between years is relatively small as much of the annual precipitation is evaporated and thus has little effect in altering water storage. For example, Ning et al. (2017) argued that a one-year aggregated time period is appropriate in the semi-arid Loess Plateau; 2) the carryover of soil water storage would result in an overestimated E , and in turn an overestimated n . The catchment NO.10 had a medium n value (1.7) in the reference period, much smaller than the evaluation period (4.2). If the 3-year data period had caused a bias, the real value of the n change would be larger. Hence, the largest changes in n cannot be related to the 3-year data period.

11. [Figure 6: It is unclear what is shown here.]

Figure 6 has become Figure 8 in the revised version.

The figure compares the temporal variability of the sensitivities of R to P , E_0 , and n . The boxplot clearly showed that the sensitivities to n is greatest, so it is unreliable to predict future catchment effects using earlier sensitivity (Lines 271-278).

12. [The motivation of the figures 7,8 and 9 is not really clear to me. Please explain or remove]

They have become Figures 9, 10 and 11 in the revised version, respectively.

The manuscript re-defines the widely-used sensitivity at a point as the path-averaged sensitivity. It is worthwhile to explore the predictability of the path-averaged sensitivity. All of the figures are for this aim. I am sorry I do not remove them.

Fig. 9 shows the correlation between the obtained sensitivities and P , E_0 , n , and aridity index, for purpose to determine the predictors of the sensitivities, which

will be used in Fig. 11.

Fig. 10 shows that the spatial predictions of the path-averaged sensitivities is easy if having the long-term mean values of P , E_0 , and R .

I used the predictors that was determined in Fig. 9 to predict the path-averaged sensitivities. Fig. 11 shows the prediction performance.

13. [At Line 311-312 it is argued that the timing of precipitation change is important. I did not see this aspect in the results.]

This sentence is problematic. I have removed it.

Reference

Zhou, S., B. Yu, L. Zhang, Y. Huang, M. Pan, and G. Wang (2016), A new method to partition climate and catchment effect on the mean annual runoff based on the Budyko complementary relationship. *Water Resources Research*, 52, 7163–7177. <https://doi.org/10.1002/2016WR019046>, 2016.

Ning, T., Li, Z., and W. Liu: Vegetation dynamics and climate seasonality jointly control the interannual catchment water balance in the Loess Plateau under the Budyko framework, *Hydrology and Earth System Sciences*, 21, 1515-1526. <https://doi.org/10.5194/hess-2016-484>, 2017.

A line integral-based and mathematically-precise method to partition climate and catchment effects on runoff

Mingguo Zheng^{1, 2*}

¹Guangdong Key Laboratory of Integrated Agro-environmental Pollution Control and Management/
Guangdong Engineering Center of Non-point Source Pollution Prevention Technology, Guangdong
Institute of Eco-environment Science & Technology, Guangzhou 510650, China

²National-Regional Joint Engineering Research Center for Soil Pollution Control and Remediation in
South China, Guangzhou 510650, China;

³Guangdong Engineering Center of Non-point Source Pollution Prevention Technology, Guangzhou
510650, China;

Correspondence: Mingguo Zheng (mgzheng@soil.gd.cn)

Abstract

It is a common task to partition the synergistic impacts of ~~a number of~~ drivers in the environmental sciences. However, there is no mathematically precise solution to this partition process. Here I presented a line integral-based method, which ~~concerns about~~addresses the sensitivity to the drivers throughout their evolutionary ~~paths~~ so as to ensure a precise partition. The method reveals that the partition depends on both the change magnitude and pathway (timing of the change), ~~and but~~ not on the magnitude alone unless used for a linear system. To illustrate this method, I used the Budyko framework to partition the effects of climatic and catchment conditions on the temporal change in the runoff for 21 catchments from Australia and China. The proposed method ~~reduced~~reduces to the decomposition method when assuming a path ~~along in~~ which climate change occurs first, followed by an abrupt change in catchment properties. The proposed method re-defines the widely-used ~~concept of~~ sensitivity at a point as the path-averaged sensitivity. The total differential and the complementary methods simply concern ~~about~~ the sensitivity at the initial or/and the terminal state, so ~~that~~ they cannot give precise results. The path-averaged sensitivity of water yield to climate conditions was found to be stable over time. Space-wise, moreover, the sensitivity ~~it~~ can be readily predicted even in the absence of streamflow observations, ~~whereby which~~ facilitates the evaluation of future climate effects on streamflow. As a mathematically accurate solution, the proposed method provides a generic tool to conduct ~~the~~ quantitative attribution analyses.

Keywords: Runoff; Climate change; Human activities; Attribution analysis; Budyko

1 Introduction

The impacts of certain drivers on observed changes of interest often require quantification in environmental sciences. In the hydrology community, both climate and human activities have posed global-scale impact on hydrologic cycle and water resources (Barnett *et al.*, 2008; Xu *et al.*, 2014; Wang

设置了格式: 字体颜色: 自动设置

设置了格式: 字体: (默认) Times New Roman, (中文)
Calibri, 字体颜色: 自动设置

设置了格式: 字体颜色: 自动设置

40 ~~and Hejazi, 2001). Diagnosing their relative contributions to runoff is of considerable relevance to the~~
41 ~~researchers and managers. It is often needed to quantify the relative roles of a few drivers to the observed~~
42 ~~changes of interest in environmental sciences. In the hydrology community, diagnosing the relative~~
43 ~~contributions of climate change and human activities to runoff is of great relevance to the researchers and~~
44 ~~managers as both climate and human activities have pose global scale impact on hydrologic cycle and~~
45 ~~water resources (Barnett *et al.*, 2008; Xu *et al.*, 2014; Wang and Hejazi, 2001). Unfortunately, performing~~
46 ~~a the~~ quantitative attribution analysis of ~~the~~ runoff changes remains a challenge (Wang and Hejazi, 2001;
47 Berghuijs and Woods, 2016; Zhang *et al.*, 2016); this is to a considerable degree due to a lack of a
48 mathematically precise method to decouple synergistic and often confounding impacts of climate change
49 and human activities.

50
51 Numerous studies have detected the long-term variability in runoff and attempted to partition the
52 effects of climate change and human activities ~~through by means of~~ various methods (Dey and Mishra,
53 2017); ~~these include. Among them are~~ the paired-catchments method and the hydrological modeling
54 method. The paired-catchment method ~~is believed to be able to can~~ filter the effect of climatic variability
55 and thus isolate the runoff change induced by vegetation changes (Brown *et al.*, 2005). However, ~~thise~~
56 method is capital intensive; ~~moreover, . Particularly,~~ it generally involves small catchments and
57 ~~experiences difficulties is challenged~~ when extrapolating to large catchments (Zhang *et al.*, 2011). The
58 physical-based hydrological models often ~~suffer from have~~ limitations ~~including such as a~~ high data
59 requirement, labor-intensive calibration and validation processes, and inherent uncertainty and
60 interdependence in parameter estimations (Binley *et al.*, 1991; Wang *et al.*, 2013; Liang *et al.*, 2015).
61 ~~Conceptual models such as Budyko-type equations have consequently gained interest in recent~~
62 ~~years. Interest then turns to the conceptual models over recent years, such as the Budyko type equations~~
63 (see Section 2.1).

64 Within the Budyko framework, ~~a large number of~~ studies (Roderick and Farquhar, 2011; Zhang
65 *et al.*, 2016) have used the total differential of runoff (~~i.e. dR , where R represents runoff~~) as a proxy for
66 the runoff change (~~i.e. ΔR~~) and ~~the partial derivatives as the sensitivities further evaluated hydrological~~
67 ~~responses to climate change and human activities~~ (hereafter called the total differential method). ~~The total~~
68 ~~differential, however, is simply a first-order approximation of the observed change (Fig. 1(a)). This~~
69 ~~approximation has caused an error in the calculation of climate impact on runoff, with the deviation~~
70 ~~ranging from 0 to 20 10^{-3} m (or -118 to 174%) in China (Yang *et al.*, 2014). However, dR is essentially a~~
71 ~~first order approximation of ΔR (Fig. 1(a)). It has been shown that the approximation has caused an error~~
72 ~~of the climate impact on runoff ranging from 0 to 20 mm (or -118 to 174%) over China (Yang *et al.*,~~
73 ~~2014). The total differential method directly used the partial derivatives of runoff as the sensitivities of~~
74 ~~runoff to climate and catchment conditions. Most studies applied the forward approximation of the runoff~~
75 ~~change, i.e., using the sensitivities at the initial state while calculation (e.g. Roderick and Farquhar, 2011).~~
76 The elasticity method proposed by Schaake (1990) is also based on the total differential expression
77 (Sankarasubramanian *et al.*, 2001; Zheng *et al.*, 2009). The method uses the “elasticity” concept to assess
78 the climate sensitivity of runoff. The elasticity coefficients, however, have been estimated in an empirical
79 way and ~~is-are~~ not physically sound (Roderick and Farquhar, 2011; Liang *et al.*, 2015).

80 The so-called decomposition method developed by Wang and Hejazi (2011) has also been widely
81 used. The method assumes that climate changes ~~drive cause~~ a shift along a Budyko curve and then human

批注 [A1]: Kindly ensure that the revision retains the intended meaning of the sentence.

interferences cause a vertical shift from ~~the one~~ Budyko curve to another (Fig. 4(b)). Under this assumption, the method extrapolates the Budyko models that are calibrated using observations of the reference period, in which human impacts remain minimal, to determine the human-induced runoff changes ~~in runoff that occurred~~ during the evaluation period.

Recently, Zhou *et al.* (2016) established a Budyko complementary relationship for runoff and further applied it to partitioning the climate and catchment effects. Superior to the total differential method, the complementary method culminates with-by yielding a no-residual partition. Nevertheless, ~~the this~~ method depends on a given weighted factor ~~that-which~~ is determined in an empirical but not a precise way. Furthermore, Zhou *et al.* (2016) argued that the partition is not unique in the Budyko framework ~~as~~ because the path of the climate and catchment changes cannot be uniquely identified.

A ~~Obtaining~~ a precise partition remains difficult, even when using given a precise mathematical model. This difficulty can be illustrated by using a precise hydrology model $R = f(x, y)$, where R represents runoff, and x and y represent the climate factors and catchment characteristics, respectively. We assumed that R ~~changes~~ changes by ΔR when x ~~changes~~ changed by Δx and y changes by Δy , *i.e.*, $\Delta R = f(x + \Delta x, y + \Delta y) - f(x, y)$. To determine the effect of x on ΔR , ~~ΔR~~ , *i.e.* ΔR_x , a common practice is to assume that y remains constant when x changes by Δx . We thus ~~get~~ obtain: $\Delta R_x = f(x + \Delta x, y) - f(x, y)$. Similarly, we can ~~get~~ obtain: $\Delta R_y = f(x, y + \Delta y) - f(x, y)$. Although ~~the this~~ derivation seems quite reasonable, it is problematic as ~~the sum of $\Delta R_x + \Delta R_y \neq \Delta R$ and ΔR_y is not equal to ΔR~~ . A ~~F~~ further examination shows that a variable's effect on R seems to differ depending on the changing path (timing of the change). For example, $\Delta R_x = f(x + \Delta x, y) - f(x, y)$ and $\Delta R_y = f(x + \Delta x, y + \Delta y) - f(x + \Delta x, y)$ if x changes first and y subsequently changes (Note that the partition is precise with $\Delta R_x + \Delta R_y = \Delta R$ at this moment ~~the sum of ΔR_x and ΔR_y equaling ΔR now~~). If y changes first and x subsequently changes, the partition then becomes: $\Delta R_x = f(x + \Delta x, y + \Delta y) - f(x, y + \Delta y)$ and $\Delta R_y = f(x, y + \Delta y) - f(x, y)$. In the case of x and y changing simultaneously, unfortunately, current literature seems not to provide a mathematically precise solution.

The ~~aims~~ of this work-study are-is to propose a mathematically precise method to conduct a quantitative attribution to drivers. The method is based on the line integral (called the LI method hereafter) and takes account of the sensitivity throughout the evolutionary path of the drivers rather than at a point as the total differential method does. In this way, the proposed method revises the widely-used concept of sensitivity at a point as the path-averaged sensitivity. To present and evaluate the proposed method, I decomposed the relative influences of climate and catchment conditions on runoff within the Budyko framework using data from 21 catchments from Australia and China. I also examined the spatio-temporal variability of the path-averaged sensitivities ~~of runoff to climatic and catchment conditions~~ and assessed their spatio-temporal predictability.

设置了格式: 字体: 倾斜

设置了格式: 字体: (默认) Times New Roman, (中文) Calibri

域代码已更改

域代码已更改

2 Methodology

2.1 The Budyko Framework and the MCY equation

Budyko (1974) argued that the mean annual evapotranspiration (E) is largely determined by the water and energy balance of a catchment. Using precipitation (P) and potential evapotranspiration (E_0) as proxies for water and energy availabilities respectively, the Budyko framework relates evapotranspiration losses to the aridity index defined as the ratio of E_0 over P . The Budyko framework has gained wide acceptance in the hydrology community (Berghuijs and Woods, 2016; Sposito, 2017). In recent or past decades, several equations have been developed to describe the Budyko framework. Among them, the Mezentsev-Choudhury-Yang's equation (Mezentsev, 1955; Choudhury, 1999; Yang *et al.*, 2008) (Called the MCY equation hereafter) has been widely accepted and was used in this study here:

$$\frac{E}{P} = \frac{E_0/P}{(1 + (E_0/P)^n)^{1/n}} \quad (1)$$

where $n \in (0, \infty)$ is an integration constant that is dimensionless, and represents catchment properties. Eq. (3) requires a relatively long time scale whereby the water storage of a catchment is negligible and the water balance equation reduces to be $R = P - E$. Here I adopted a "tuned" n value that can obtain an exact accordance between the calculated E by Eq. (1) and that actually encountered ($= P - R$).

The partial differentials of R with respect to P , E_0 , and n are given as:

$$\frac{\partial R}{\partial P} = R_P(P, E_0, n) = 1 - \frac{E_0^{n+1}}{(P^n + E_0^n)^{1/n}} \quad (2a)$$

$$\frac{\partial R}{\partial E_0} = R_{E_0}(P, E_0, n) = -\frac{P^{n+1}}{(P^n + E_0^n)^{1/n}} \quad (2b)$$

$$\frac{\partial R}{\partial n} = R_n(P, E_0, n) = \frac{-E_0 P n^{-1}}{(P^n + E_0^n)^{1/n}} \left[\frac{\ln(P^n + E_0^n)}{n} - \frac{P^n \ln P + E_0^n \ln E_0}{P^n + E_0^n} \right] \quad (2c)$$

2.2 The theory of the line integral-based method

To present the LI method, we start by considering an example of a two-variable function $z = f(x, y)$. The which function has continuous partial derivatives $\partial z / \partial x = f_x(x, y)$ and $\partial z / \partial y = f_y(x, y)$ and we assumed that x and y are independent. Suppose that x and y varies along a smooth curve L (e.g. AC in Fig. 1(e) Fig. 3) from the initial state (x_0, y_0) to the terminal state (x_N, y_N) , and z co-varies from z_0 to z_N . Let $\Delta z = z_N - z_0$, $\Delta x = x_N - x_0$, and $\Delta y = y_N - y_0$. Our goal is to seek for determine a mathematical solution to that quantify the effects of Δx and Δy on Δz , i.e. Δz_x and Δz_y . Δz_x and Δz_y should be subject to the constraint $\Delta z_x + \Delta z_y = \Delta z$.

As shown in Fig. 1(e) Fig. 3, points $M_1(x_1, y_1), \dots, M_{N-1}(x_{N-1}, y_{N-1})$ partition L into N distinct segments. Let $\Delta x_i = x_{i+1} - x_i$, $\Delta y_i = y_{i+1} - y_i$, and $\Delta z_i = z_{i+1} - z_i$. For each segment, Δz_i can be approximated as the total differential $d z_i$: $\Delta z_i \approx d z_i = f_x(x_i, y_i) \Delta x_i + f_y(x_i, y_i) \Delta y_i$. We then have:

设置了格式: 字体: (默认) Times New Roman, (中文) Calibri

设置了格式: 字体: (默认) Times New Roman, (中文) Calibri

设置了格式: 字体: 小四

设置了格式: 字体: 小四, 倾斜

设置了格式: 字体: 小四

设置了格式: 字体: 小四, 倾斜

设置了格式: 字体: 小四

设置了格式: 字体: 倾斜

149 $\Delta z = \sum_{i=1}^N \Delta z_i \approx \sum_{i=1}^N f_x(x_i, y_i) \Delta x_i + \sum_{i=1}^N f_y(x_i, y_i) \Delta y_i$. We thus obtain ~~an~~ the following respective approximation
 150 of Δz_x and Δz_y : $\Delta z_x \approx \sum_{i=1}^N f_x(x_i, y_i) \Delta x_i$ and $\Delta z_y \approx \sum_{i=1}^N f_y(x_i, y_i) \Delta y_i$. ~~Next, D~~ Define τ as the maximum length
 151 among the N segments. The smaller the value of τ , the closer to Δz_i the value of ~~d~~ Δz_i , and then the more
 152 accurate ~~better~~ the approximations are. The approximations becomes exact in the limit $\tau \rightarrow 0$. Taking the
 153 limit $\tau \rightarrow 0$ then turns-converts the sum into integrals and gives a precise expression (~~#-this~~ is an informal
 154 derivation and please see Appendix A for a formal one):

155
$$\Delta z = \lim_{\tau \rightarrow 0} \sum_{i=1}^N f_x(x_i, y_i) \Delta x_i + \lim_{\tau \rightarrow 0} \sum_{i=1}^N f_y(x_i, y_i) \Delta y_i = \int_L f_x(x, y) dx + \int_L f_y(x, y) dy$$
, where

156 $\int_L f_x(x, y) dx = \lim_{\tau \rightarrow 0} \sum_{i=1}^N f_x(x_i, y_i) \Delta x_i$ and $\int_L f_y(x, y) dy = \lim_{\tau \rightarrow 0} \sum_{i=1}^N f_y(x_i, y_i) \Delta y_i$ denote the line integral of f_x and f_y
 157 along L (termed integral path) with respect to x and y , respectively. $\int_L f_x(x, y) dx$ and $\int_L f_y(x, y) dy$ exist
 158 provided that f_x and f_y are continuous along L . We thus obtain a precise evaluation of Δz_x and Δz_y :

159
$$\Delta z_x = \int_L f_x(x, y) dx \quad (3a)$$

160
$$\Delta z_y = \int_L f_y(x, y) dy \quad (3b)$$

161 Unlike the total differential method, the sum of Δz_x and Δz_y persistently equals Δz (Appendix B).
 162 If $f(x, y)$ is linear, then f_x and f_y are constant. ~~Define~~ Defining $C_x = f_x(x, y)$ and $C_y = f_y(x, y)$ remain constant
 163 at C_x and C_y respectively, then we have $\Delta z_x = C_x \Delta x$ and $\Delta z_y = C_y \Delta y$. Δz_x and Δz_y are thus independent of L .
 164 If $f(x, y)$ is non-linear, however, both Δz_x and Δz_y varies-vary with L , as was-is exemplified in Appendix
 165 C. Hence, the initial and the terminal states, together with the path connecting them, determine the
 166 resultant partition unless $f(x, y)$ is linear.

167 The mathematical derivation above applies to a three-variable function as well. By doing the line
 168 integrals for the MCY equation, we obtain the desired results:

169
$$\Delta R_P = \int_L \frac{\partial R}{\partial P} dP \quad (4a)$$

170
$$\Delta R_{E_0} = \int_L \frac{\partial R}{\partial E_0} dE_0 \quad (4b)$$

171
$$\Delta R_n = \int_L \frac{\partial R}{\partial n} dn \quad (4c)$$

172 where ΔR_P , ΔR_{E_0} , and ΔR_n ~~ΔR_P , ΔR_{E_0} , and ΔR_n~~ denotes the effects on runoff change of P , E_0 , and n ,
 173 respectively. The sum of ΔR_P , ΔR_{E_0} , and ΔR_n ~~ΔR_P , ΔR_{E_0} , and ΔR_n~~ represents the effect of climate change, and ΔR_n ~~ΔR_n~~
 174 are-is often related to human activities although it probably-probably includes the effects of other factors,
 175 such as climate seasonality (Roderick and Farquhar, 2011; Berghuijs and Woods, 2016). L denotes a
 176 three-dimensional curve along which climate and catchment changes have occurred. I approximated L as

域代码已更改
 设置了格式: 字体: (默认) Times New Roman
 域代码已更改
 域代码已更改
 域代码已更改
 域代码已更改
 域代码已更改
 域代码已更改

177 a union of by a series of line segments. ΔR_p , ΔR_{E_0} , and ΔR_n were finally figured
 178 out determined by summing up the integrals along each of the line segments (see Section 2.3).

179 2.3 Using the LI method to determine ΔR_p , ΔR_{E_0} , and ΔR_n within the Budyko
 180 Framework

181 1) Determining ΔR_p , ΔR_{E_0} , and ΔR_n assuming a linear integral path
 182 integral path

183 Given two consecutive periods and assumed assuming that the catchment state has evolved from
 184 (P_1, E_{01}, n_1) to (P_2, E_{02}, n_2) along a straight line L . Let $\Delta P = P_2 - P_1$, $\Delta E_0 = E_{02} - E_{01}$, and $\Delta n = n_2 - n_1$;
 185 $\Delta n = n_2 - n_1$; then the line L is given by parametric equations: $P = \Delta Pt + P_1$, $E_0 = \Delta E_0 t + E_{01}$, $n = \Delta n t + n_1$,
 186 $t \in [0,1]$. Given these equations, Eq. (2) becomes a univariate function one variable function of t , i.e.,
 187 $\partial R / \partial P = R_p(t)$, $\partial R / \partial E_0 = R_{E_0}(t)$, and $\partial R / \partial n = R_n(t)$. Then, ΔR_p , ΔR_{E_0} , and ΔR_n can be
 188 evaluated as:

$$189 \Delta R_p = \int_L \frac{\partial R}{\partial P} dP = \int_0^1 R_p(t) d(\Delta Pt + P_1) = \Delta P \int_0^1 R_p(t) dt \quad (5a)$$

$$190 \Delta R_{E_0} = \int_L \frac{\partial R}{\partial E_0} dE_0 = \int_0^1 R_{E_0}(t) d(\Delta E_0 t + E_{01}) = \Delta E_0 \int_0^1 R_{E_0}(t) dt \quad (5b)$$

$$191 \Delta R_n = \int_L \frac{\partial R}{\partial n} dn = \int_0^1 R_n(t) d(\Delta n t + n_1) = \Delta n \int_0^1 R_n(t) dt \quad (5c)$$

192 Unfortunately, I could not figure out determine the antiderivatives of $R_p(t) dt$, $R_{E_0}(t) dt$ and
 193 $R_n(t) dt$. $R_p(t)$, $R_{E_0}(t)$, and $R_n(t)$ and have had to make approximate calculations. As the discrete equivalent
 194 of integration is a summation, we can approximate the integration as a summation. I divided the $t \in [0,1]$
 195 interval into 1000 subintervals of the same width, thereby i.e., setting dt identically equal to 0.001, and
 196 then then calculated $R_p(t) dt$, $R_{E_0}(t) dt$ and $R_n(t) dt$ for each subinterval. Let
 197 $t_i = 0.001i, i \in [0,999]$ and is integer-valued, ΔR_p , ΔR_{E_0} , and ΔR_n were approximated as:

$$199 \Delta R_p \approx 0.001 \Delta P \sum_{i=0}^{999} R_p(t_i) \quad (6a)$$

$$200 \Delta R_{E_0} \approx 0.001 \Delta E_0 \sum_{i=0}^{999} R_{E_0}(t_i) \quad (6b)$$

$$201 \Delta R_n \approx 0.001 \Delta n \sum_{i=0}^{999} R_n(t_i) \quad (6c)$$

202 2) Dividing the evaluation period into a number of subperiods

203 I first determined a change point and divided the whole observation period into the reference and
 204 evaluation periods. To determine the integral path, the evaluation period is further divided into a
 205 number of subperiods. The Budyko framework assumes a steady state condition of a catchment and
 206 therefore requires no change in soil water storage. Over a time period of a time period of 5-10 years, it is
 207 reasonable to assume that changes in soil water storage are will be sufficiently small (Zhang et al., 2001).

域代码已更改

域代码已更改

域代码已更改

域代码已更改

域代码已更改

域代码已更改

域代码已更改

域代码已更改

域代码已更改

域代码已更改

域代码已更改

域代码已更改

域代码已更改

域代码已更改

域代码已更改

域代码已更改

域代码已更改

域代码已更改

域代码已更改

域代码已更改

域代码已更改

域代码已更改

域代码已更改

域代码已更改

域代码已更改

域代码已更改

域代码已更改

域代码已更改

域代码已更改

域代码已更改

域代码已更改

域代码已更改

域代码已更改

域代码已更改

域代码已更改

208 Here, I divided the evaluation period into a number of 7-year subperiods with the exception for the ~~last~~
209 ~~final~~ ~~onesubperiod~~, which varied from 7 to 13 years in length depending on the length of the evaluation
210 period.

211 3) Determining ΔR_P , ΔR_{E_0} , and ΔR_n ~~ΔR_P , ΔR_{E_0} , and ΔR_n~~ by approximating the integral path as a series
212 of line segments

213 ~~As did in Fig. 1(e), a~~ curve can be approximated as a series of line segments. For a short period,
214 the integral path L can be considered as linear, which implies a temporally invariant change rate. For a
215 long period, in which the change rate ~~usually may varies vary~~ over time, L can be fitted using a number
216 of line segments. Given a reference period and an evaluation period comprising N subperiods, I assumed
217 that the catchment state evolved from $(P_0, E_{00}, n_0), \dots, (P_i, E_{0i}, n_i), \dots$ to (P_N, E_{0N}, n_N) , where the subscript
218 "0" ~~denotes denotes~~ the reference period, and "i" and "N" ~~denotes denote~~ the i th and the ~~last-final~~
219 subperiods of the evaluation period, respectively. I used a series of line segments L_1, L_2, \dots, L_N to
220 approximate the integral path L , where L_i connects $(P_{i-1}, E_{0,i-1}, n_{i-1})$ with (P_i, E_{0i}, n_i) , ~~and the initial point of L_{i+1} is the terminal point of L_i and~~ Then ΔR_P , ΔR_{E_0} , and
221 ΔR_n ~~were evaluated as the sum of the integrals along each of the line segments ΔR_P , ΔR_{E_0} , and ΔR_n are~~
222 ~~evaluated as the sum of the integrals along each of the line segments~~, which ~~was were~~ calculated using
223 Eq. (6).
224

225 2.4 ~~The~~ total-differential, decomposition and complementary methods

226 To evaluate the LI method, I compared it with the decomposition method, the total differential
227 method, and the complementary method. The total differential method approximated ΔR ~~ΔR~~ as ~~dR~~ (Fig.
228 ~~(a))~~:

$$229 \Delta R \approx dR = \frac{\partial R}{\partial P} \Delta P + \frac{\partial R}{\partial E_0} \Delta E_0 + \frac{\partial R}{\partial n} \Delta n = \lambda_P \Delta P + \lambda_{E_0} \Delta E_0 + \lambda_n \Delta n \quad (7)$$

230 where $\lambda_P = \partial R / \partial P$, $\lambda_{E_0} = \partial R / \partial E_0$, and $\lambda_n = \partial R / \partial n$, representing the sensitivity coefficient of R with respect
231 to P , E_0 , and n , respectively. Within the total differential method, $\Delta R_P = \lambda_P \Delta P$, $\Delta R_{E_0} = \lambda_{E_0} \Delta E_0$, and
232 $\Delta R_n = \lambda_n \Delta n$. I used the forward approximation, *i.e.*, substituting the observed mean annual values of the
233 reference period into Eq. (2), to estimate λ_P , λ_{E_0} , and λ_n , as ~~is standard~~ in most studies (Roderick and
234 Farquhar, 2011; Yang and Yang, 2011; Sun *et al.*, 2014).

235 The decomposition method (Wang and Hejazi, 2011) calculated ΔR_n ~~ΔR_n~~ as follows:

$$236 \Delta R_n = R_2 - R'_2 = (P_2 - E_2) - (P_2 - E'_2) = E'_2 - E_2 \quad (8)$$

237 where R_2 , P_2 , and E_2 represents the mean annual runoff, precipitation and evapotranspiration of the
238 evaluation period, ~~respectively~~; and R'_2 and E'_2 represents the mean annual runoff and evapotranspiration,
239 respectively, given the climate conditions of the evaluation period and the catchment conditions of the
240 reference period. Both E_2 and E'_2 were calculated by Eq. (1), but using n values of the evaluation period
241 and the reference period respectively.

242 The complementary method (Zhou *et al.*, 2016) uses a linear combination of the complementary
243 relationship for runoff to determine ΔR_P , ΔR_{E_0} , and ΔR_n ~~ΔR_P , ΔR_{E_0} , and ΔR_n~~ :

域代码已更改

域代码已更改

域代码已更改

域代码已更改

设置了格式: 字体: (默认) Times New Roman

域代码已更改

设置了格式: 字体: (默认) Times New Roman

域代码已更改

域代码已更改

域代码已更改

域代码已更改

域代码已更改

域代码已更改

244

$$\Delta R = a \left[\left(\frac{\partial R}{\partial P} \right)_1 \Delta P + \left(\frac{\partial R}{\partial E_0} \right)_1 \Delta E_0 + P_2 \Delta \left(\frac{\partial R}{\partial P} \right) + E_{0,2} \Delta \left(\frac{\partial R}{\partial E_0} \right) \right] \quad (9)$$

$$+ (1-a) \left[\left(\frac{\partial R}{\partial P} \right)_2 \Delta P + \left(\frac{\partial R}{\partial E_0} \right)_2 \Delta E_0 + P_1 \Delta \left(\frac{\partial R}{\partial P} \right) + E_{0,1} \Delta \left(\frac{\partial R}{\partial E_0} \right) \right]$$

245

246

247

where the subscript 1 and 2 denotes the reference and the evaluation periods, respectively. a is a weighting factor and varies from 0 to 1. As suggested by Zhou *et al.* (2016), I set $a = 0.5$. Equation (9) thus gave an estimation of ΔR_p , ΔR_{E_0} , and ΔR_n . ~~ΔR_p , ΔR_{E_0} , and ΔR_n~~ as follows:

248

$$\Delta R_p = 0.5 \Delta P \left[\left(\frac{\partial R}{\partial P} \right)_1 + \left(\frac{\partial R}{\partial P} \right)_2 \right] \quad (10a)$$

249

$$\Delta R_{E_0} = 0.5 \Delta E_0 \left[\left(\frac{\partial R}{\partial E_0} \right)_1 + \left(\frac{\partial R}{\partial E_0} \right)_2 \right] \quad (10b)$$

250

$$\Delta R_n = 0.5 \Delta \left(\frac{\partial R}{\partial P} \right) (P_1 + P_2) + 0.5 \Delta \left(\frac{\partial R}{\partial E_0} \right) (E_{0,1} + E_{0,2}) \quad (10c)$$

251

2.5 Data

252

253

254

255

256

257

258

259

260

261

262

263

264

265

266

267

268

269

270

271

272

273

274

275

I collected ~~data of~~ runoff and climate ~~data of from~~ 21 selected catchments ~~from evaluated in~~ previous studies (Table 1). The change-point years ~~gave given~~ in these ~~was were~~ directly used to determine the reference and evaluation periods for the LI method. As mentioned above, the LI method further divides the evaluation period into a number of subperiods. For the sake of comparison, the ~~last final~~ subperiod of the evaluation period was used as the evaluation period for the decomposition, the total differential and the complementary methods (It can be equally considered that all ~~of the four~~ methods used the ~~last final~~ subperiod as the evaluation period, but the LI method cares about the intermediate period between the reference and the evaluation periods and the other ~~methodss~~ do not). Nine of the 21 catchments had a reference period comprising only one subperiod (Table 1), and the others had two to seven ~~onesubperiods~~.

The 21 selected catchments ~~were located in~~ have diverse climates and landscapes ~~with~~. Among ~~them~~, 14 ~~are~~ from Australia and ~~7 seven~~ from China (Table 1). The catchments ~~spanned spans~~ from tropical to subtropical and temperate ~~areas~~ and from humid to semi-humid and semi-arid regions, with ~~the~~ mean annual rainfall varying from 506 to 1014 ~~10⁻³m mm~~ and potential evaporation from 768 to 1169 ~~10⁻³m mm~~. The ~~index of dryness index~~ ranges between 0.86 and 1.91. The catchment areas vary by five orders of magnitude from 1.95 to 121,972 with a median 606 ~~10⁹km²~~. The key data includes annual runoff, precipitation, and potential evaporation. The record length varied between 15 and 75 with a median of 35 years. Among the 21 catchments, the changes from the reference to the evaluation period ranged between -271 and 79 ~~10⁻³m mm~~ yr⁻¹ for precipitation, and ~~between~~ -35 and 41 ~~10⁻³m mm~~ yr⁻¹ for potential evaporation (Table 2). The coeal change in the parameter n of the MCY equation ranged between -0.2 to 2.53. All ~~of the~~ catchments experienced ~~changes both in~~ climate ~~change and~~ ~~catchment properties~~ ~~and~~ ~~cover change~~ over the observation periods. The mean annual streamflow reduced for all ~~of the~~ catchments, ~~by ranging~~ from 0.43 to 229 with a median 38 ~~10⁻³m mm~~ yr⁻¹. ~~For all catchments, the~~ ~~change in catchment properties mainly refer to the vegetation cover or land use change~~. More details of

域代码已更改

域代码已更改

域代码已更改

设置了格式: 字体: (默认) Times New Roman, (中文) Calibri

276 data and the catchments can be found in Zhang *et al.* (2011), Sun *et al.* (2014), Zhang *et al.* (2010), Zheng
277 *et al.* (2009), Jiang *et al.* (2015), and Gao *et al.* (2016).

279 3 Results

280 3.1 Comparisons with existing methods

281 ~~The LI method first partitions the whole observation period into the reference and evaluation~~
282 ~~periods, then further divides the latter into a number of subperiods and evaluates the contributions to~~
283 ~~runoff from climate and catchment changes for each subperiod, and finally adds up the derived~~
284 ~~contributions. Table 3 lists all of the resultant values of ΔR_p , ΔR_{E_0} , and ΔR_n . ΔR_p , ΔR_{E_0} , and ΔR_n of from the~~
285 ~~LI method and, together with the three other methods. Please see the supplemental information section~~
286 ~~for detailed calculation steps.~~

287 Fig. 2 Fig. 4(a) compares the resultant ΔR_n ~~ΔR_n~~ of the LI method and the decomposition method.
288 Although they are quite similar, the discrepancies between ~~them these values~~ can be up to $>20 \cdot 10^{-3} \text{ m mm}$
289 yr^{-1} . The decomposition method assumes that climate change occurs first and then human interferences
290 cause a sudden change in catchment properties (Fig. 1(b)2). Such a fictitious path is identical to the broken
291 line of AB+BC in Fig. 1(e) Fig. 3, provided that x represents climate factors and y catchment properties.
292 As a result, the decomposition method can be considered as a special case of the LI method when adopting
293 the broken line AB+BC ~~broken line~~ in Fig. 1(e) Fig. 3 as the integral path, as was demonstrated clearly in
294 Fig. 2 Fig. 4(b).

295 The total differentiae method is predicated on an approximate equation, *i.e.* Eq. (7). The LI method
296 reveals that the precise form of the equation is $\Delta R = \bar{\lambda}_p \Delta P + \bar{\lambda}_{E_0} \Delta E_0 + \bar{\lambda}_n \Delta n$ (~~*i.e.* Eq. (D2) in Appendix D~~),
297 where $\bar{\lambda}_p$, $\bar{\lambda}_{E_0}$, and $\bar{\lambda}_n$ (Table 4) denote the path-averaged sensitivity of R to P , E_0 , and n , respectively. All
298 points along the path have the same weight in determining $\bar{\lambda}_p$, $\bar{\lambda}_{E_0}$, and $\bar{\lambda}_n$. To determine them, the total
299 differential ~~and the complementary methods~~ utilizes only the initial ~~state or/and the complementary~~
300 ~~method utilizes the initial and the terminal states. Neglecting the intermediate states between the initial~~
301 ~~and the terminal states ones would result in an imprecise partition, as was illustrated in Fig. 1 using a~~
302 ~~univariate function, and even possibly results in a reverse trend estimation (see ΔR_{E_0} ΔR_{E_0} for Catchment~~
303 ~~NO. 1 in Table 3). Although the elasticity method exploits information contained over the entire~~
304 ~~observation period (e.g. Zheng *et al.*, 2009; Wang *et al.*, 2013), the resultant descriptive statistics of~~
305 ~~climate elasticity may not be robust (Roderick and Farquhar, 2011; Liang *et al.*, 2015).~~

306 Superior to the total differential method, the sum of ΔR_p , ΔR_{E_0} , and ΔR_n ~~ΔR_p , ΔR_{E_0} , and ΔR_n~~ always
307 equaled to ΔR ~~ΔR~~ for the LI method. Examination of the subperiods revealed that $\partial R / \partial n$ was more
308 temporally variable than $\partial R / \partial P$ and $\partial R / \partial E_0$ (discussed below). For this reason, ~~ΔR_p ΔR_n~~ showed
309 considerable discrepancies between the two methods, but ΔR_p ~~ΔR_p~~ as well as ΔR_{E_0} ~~ΔR_{E_0}~~ matched ~~well~~
310 ~~closely~~ between the two methods (Fig. 3 Fig. 5).

域代码已更改

域代码已更改

域代码已更改

设置了格式: 字体: (默认) Times New Roman, (中文) Calibri

设置了格式: 字体: (默认) Times New Roman, (中文) Calibri

域代码已更改

域代码已更改

域代码已更改

域代码已更改

域代码已更改

域代码已更改

域代码已更改

域代码已更改

域代码已更改

311 As with the LI method, the complementary method produced $\overline{\Delta R_P}$, $\overline{\Delta R_{E_0}}$, and $\overline{\Delta R_n}$. $\overline{\Delta R_P}$, $\overline{\Delta R_{E_0}}$, and
312 $\overline{\Delta R_n}$ that exactly add-summed up to $\overline{\Delta R}$. Although its resultant $\overline{\Delta R_P}$, $\overline{\Delta R_{E_0}}$, and $\overline{\Delta R_n}$ values $\overline{\Delta R_P}$, $\overline{\Delta R_{E_0}}$,
313 and $\overline{\Delta R_n}$ were all in accordance good agreement with the LI method (Fig. 4 Fig. 6), the LI method often
314 yielded values beyond the bounds given by the complementary method (Fig. 5 Fig. 7); this is because the
315 maximum or minimum sensitivities do not necessarily occur at the initial and-or terminal states. are not
316 equivalent to the maximum and minimum values over the integral path.

3.2 The λ spatio-temporal variability of the path-averaged sensitivities

317 $\overline{\lambda_P}$, $\overline{\lambda_{E_0}}$ and $\overline{\lambda_n}$ implies-implies the average runoff change induced by a unit change in P , E_0 and n ,
318 respectively (Appendix D). Their spatio-temporal variability is relevant to the prediction of the runoff
319 change. To evaluate their temporal variabilities, I calculated $\overline{\lambda_P}$, $\overline{\lambda_{E_0}}$ and $\overline{\lambda_n}$ for each subperiod of the
320 evaluation period and assessed their deviation from those for the whole evaluation period. As shown in
321 Fig. 6 Fig. 8, the deviation was rather limited for $\overline{\lambda_P}$ (averaged 8.6%) and $\overline{\lambda_{E_0}}$ (averaged 13%), but was
322 considerable for $\overline{\lambda_n}$ (averaged 41%). Hence, it seems quite safe to predict the future climate effects on
323 runoff using the earlier $\overline{\lambda_P}$ and $\overline{\lambda_{E_0}}$ values, but care must be taken when using earlier $\overline{\lambda_n}$ to predict future
324 catchment effect on runoff.

325 Different from the temporal variability, $\overline{\lambda_P}$, $\overline{\lambda_{E_0}}$ and $\overline{\lambda_n}$ all varied greatly, by up to several times
326 or even ten folds, between the studied catchments (Table 4). It was found that there were good Strong
327 correlations were observed between $\overline{\lambda_P}$ and P , between $\overline{\lambda_{E_0}}$ and P , and between $\overline{\lambda_n}$ and n (Fig. 7 Fig. 9).
328 Fig. 8 Fig. 10 shows that Eq. (2) reproduced $\overline{\lambda_P}$, $\overline{\lambda_{E_0}}$ and $\overline{\lambda_n}$ very well taking the long-term means of P ,
329 E_0 , and n as inputs, a fact that the dependent variable approached its average if setting the independent
330 variables were set to be their averages. The-This finding is of relevance to the spatial prediction of $\overline{\lambda_P}$,
331 $\overline{\lambda_{E_0}}$ and $\overline{\lambda_n}$; moreover, it would greatly facilitate the prediction of future climate effect on runoff as $\overline{\lambda_P}$
332 and $\overline{\lambda_{E_0}}$ was rather stable over time as previously mentioned.

333 Runoff data and, in turn, the parameter n in the MCY equation, are often unavailable. It is thus
334 desirable to make predictions of $\overline{\lambda_P}$, $\overline{\lambda_{E_0}}$ and $\overline{\lambda_n}$ in the absence of the parameter n . I developed three
335 strategies as follows: 1) using Eq. (2) and assuming $n = 2$ as n is typically in a small range from 1.5 to 2.6
336 (Roderick and Farquhar, 2011); 2) using P and E_0 to establish regression models; establish regression
337 models; 3) using the aridity index to establish regression establish regressions as it-the index appeared to
338 be more strongly correlated with both $\overline{\lambda_P}$ and $\overline{\lambda_{E_0}}$ than P and E_0 (Fig. 7 Fig. 9). As shown in Fig. 9 Fig. 11,
339 the three strategies have-show similar performance although the second one seems to perform better. All
340 of the strategies gave acceptable predictions of $\overline{\lambda_P}$ and $\overline{\lambda_{E_0}}$, but rather poor results for $\overline{\lambda_n}$ as- as it was
341 primarily controlled by n (Fig. 7 Fig. 9). Thus, It was thus needed to seek more sophisticated approaches
342 are needed to predict the future catchment effect on runoff in the absence of runoff observations.
343
344

域代码已更改

域代码已更改

域代码已更改

设置了格式: 字体: (默认) Times New Roman, (中文) Calibri

设置了格式: 字体: (默认) Times New Roman, (中文) Calibri

域代码已更改

域代码已更改

设置了格式: 字体: (中文) 宋体, 小四, 字体颜色: 黑色

设置了格式: 字体: (中文) 宋体, 字体颜色: 黑色

域代码已更改

设置了格式: 字体: (中文) 宋体, 字体颜色: 黑色

域代码已更改

4 Discussion

The LI method re-defines the widely used concept of sensitivity at a point as the path averaged sensitivity. The LI method highlights the role of the evolutionary path in determining the resultant partition. Yet, it seems that no studies have taken into account accounted for the path issue while evaluating the relative influences of drivers. Compared with the existing methods, the limit of the LI method is high data requirement for obtaining the evolutionary path. When the data are unavailable, the complementary method can be considered as an alternative. First, the complementary complementary method offer results free of residuals; in addition moreover, it employs both data of the reference and the evaluation periods to determine the sensitivities, thereby generally yielding sensitivities values closer to the path-averaged sensitivities results than the total differentiae method.

While using the Budyko models, a reasonable time scale is relevant to meet the assumption that changes in catchment water storage are small relative to the magnitude of fluxes of P , R and E (Donohue *et al.*, 2007; Roderick and Farquhar, 2011). A seven-year time scale was used in the present study, as the present study selected seven years as most studies have suggested that a time period of 5-10 years (Zhang *et al.*, 2001; Zhang *et al.*, 2016; Wu *et al.*, 2017a; Wu *et al.*, 2017b; Li *et al.*, 2017) or even one year (Roderick and Farquhar, 2011; Sivapalan *et al.*, 2011; Carmona *et al.*, 2014; Ning *et al.*, 2017) is reasonable. Nevertheless, some studies argued asserted that the time period should be longer than ten years (Li *et al.*, 2016; Dey and Mishra, 2017). If this is the case, the high temporal variation of λ_n shown in Fig. 6 Fig. 8 might be caused by water storage changes, rather than actual changes in the catchment properties. The This uncertainty should be addressed. Using the Gravity Recovery and Climate Experiment (GRACE) satellite gravimetry, Zhao *et al.* (2011) detected the water storage variations for three largest river basins of China, namely, the Yellow, Yangtze, and Zhujiang. The Yellow River mostly drains an arid and semiarid region (P , 450 mm 10^{-3} m; R , 70 10^{-3} m; E , 380 10^{-3} m), and the Yangtze (P , 110 10^{-3} m; R , 550 10^{-3} m; E , 550 mm $550 \cdot 10^{-3}$ m) and the Zhujiang river basins (P , 1400 10^{-3} m; R , 780 10^{-3} m; E , 620 10^{-3} m) are humid. The amplitude of the water storage variations between years were 7, 37.2 and 65 10^{-3} m for the three rivers respectively, at one magnitude order smaller than the fluxes of P , R and E . Although the observations cannot be directly extrapolated to other regions, the possibility seems remote that the use of a 7-year aggregated time strongly violates the assumption of the steady state condition.

The mutual independence between the drivers is crucial for a valid partition. In the present study, although annual P and E_0 exhibited significant correlation for most catchments ($p < 0.05$), the aggregated P , E_0 and n over a 7-year period showed minimal correlation (mostly $p > 0.1$). The interdependence between the drivers can considerably confound the resultant partitions of the LI method and other existing methods.

The LI method re-defines the widely-used concept of sensitivity at a point as the path-averaged sensitivity. Mathematically, the LI method is unrelated to a functional form and applies to communities other than just hydrology. For example, identifying the carbon emission budgets (an allowable amount of anthropogenic CO₂ emission consistent with a limiting warming target), is crucial for global efforts to mitigate climate change. The LI method suggested that the emission budgets depends on both the emission magnitude and pathway (timing of emissions), which is in line with a recent study by Gasser *et al.* (2018).

设置了格式: 突出显示

设置了格式: 字体: 倾斜

带格式的: 缩进: 首行缩进: 0 字符

设置了格式: 非突出显示

385 Hence, an optimal pathway would ~~bring about~~facilitate an elevated carbon budget unless the carbon-
386 climate system behaves in a linear fashion.

387 This study presented the LI method using time-series data, but it applies equally to the case of
388 spatial series of data. Given a model that relates fluvial or aeolian sediment load to the influencing factors
389 (e.g. rainfall and topography), for example, the LI method can be used to separate their contributions to
390 the sediment-load change along a river or in the along-wind direction.

391

392 5 Conclusions

393 Based on the line integral, I ~~found~~created a mathematically precise ~~solution method~~ to partition the
394 synergistic effects of ~~a number of several factors that cumulatively drive a system to change from a state~~
395 to the other. The method is relevant for quantitative assessments of the relative roles of the factors on the
396 change in the system state independent variables on the change in the dependent variable. I ~~then~~ applied
397 the LI method to partition the effects ~~on runoff~~ of climatic and catchment conditions on runoff within the
398 Budyko framework. The method reveals that in addition to the change magnitude, the change pathways
399 of climatic and catchment conditions also ~~exert~~ control ~~on~~ their impacts on runoff. Instead of using the
400 runoff sensitivity at a point, the LI method uses the path-averaged sensitivity, thereby ensuring a
401 mathematically precise partition. I further examined the spatio-temporal variability of the path-averaged
402 sensitivity. Time-wise, the runoff sensitivity to climate is stable ~~to climate~~ but that to catchment properties
403 is highly variable ~~to catchment properties~~, suggesting that ~~it is reliable to~~ predicting future climate effects
404 using earlier observations is reliable but care must be taken when predicting ~~the future~~ catchment effects.
405 Space-wise (between catchments) the runoff sensitivity both to climatic and catchment conditions was
406 highly variable ~~both to climatic and catchment conditions~~, but it can be well-accurately depicted by ~~the~~
407 long-term means of the climatic and catchment conditions. As a mathematically accurate scheme, the LI
408 method has the potential to be a generic attribution approach in the ~~the~~ environmental sciences.

409

410 Data availability

411 The data used in this study are freely available by contacting the authors.

412

413 Author contribution

414 MZ designed the study, ~~analyzing~~ analyzed the data and wrote the manuscript.

415

416 Competing interests

417 The authors declare that they have no conflict of interest.

418

带格式的: 缩进: 首行缩进: 2.5 字符

设置了格式: 字体: Times New Roman

419 **Appendix A: Mathematical proof Derivation of equation of** $\Delta z = \int_L f_x(x, y)dx + \int_L f_y(x, y)dy$

420 We define that the curve L in ~~Fig. 1(e)~~Fig. 3 is given by a parametric equation: $x = x(t)$, $y = y(t)$,
421 $t \in [t_0, t_N]$, then $\Delta z = z_N - z_0 = f[x(t_N), y(t_N)] - f[x(t_0), y(t_0)]$. Substituting the parametric equations, we
422 ~~get~~obtain:

423 The right-hand side of the equation $\equiv \int_L f_x(x, y)dx + \int_L f_y(x, y)dy$

$$424 = \int_{t_0}^{t_N} f_x[x(t), y(t)]dx(t) + \int_{t_0}^{t_N} f_y[x(t), y(t)]dy(t)$$

$$425 = \int_{t_0}^{t_N} \{f_x[x(t), y(t)]x'(t) + f_y[x(t), y(t)]y'(t)\} dt \quad (A1)$$

426 Let $g(t) = f[x(t), y(t)]$, and after using the chain rule to differentiate g with respect to t , we obtain:

$$427 g'(t) = \frac{\partial g}{\partial x} \frac{dx}{dt} + \frac{\partial g}{\partial y} \frac{dy}{dt} = f_x[x(t), y(t)]x'(t) + f_y[x(t), y(t)]y'(t) \quad (A2)$$

428 ~~It shows~~Thus, ~~that~~ $g'(t)$ is just the integrand in Eq. (A1), ~~and~~ Eq. (A1) can then be rewritten as:

429 The right-hand side of the equation $= \int_{t_0}^{t_N} g'(t) dt = [g(t)]_{t_0}^{t_N} = g(t_N) - g(t_0)$
430 $= f[x(t_N), y(t_N)] - f[x(t_0), y(t_0)] =$ The left-hand side of the equation

431 **Appendix B: The sum of $\int_L f_x(x, y)dx$ and $\int_L f_y(x, y)dy$ is path-independent**

432 **Theorem:** Given an open simply-connected region G (*i.e.*, no holes in G) and two functions $P(x, y)$
433 and $Q(x, y)$ that have continuous first-order derivatives, if and only if $\partial P / \partial y = \partial Q / \partial x$ throughout G ,
434 then $\int_L P(x, y)dx + \int_L Q(x, y)dy$ is path independent, *i.e.*, it depends solely on the starting and ending point
435 of L .

436 We have $\partial f_x / \partial y = \partial^2 z / \partial x \partial y$ and $\partial f_y / \partial x = \partial^2 z / \partial y \partial x$. As $\partial^2 z / \partial x \partial y = \partial^2 z / \partial y \partial x$, we can state that
437 $\partial f_x / \partial y = \partial f_y / \partial x$, meeting the above condition and proving that $\int_L f_x(x, y)dx + \int_L f_y(x, y)dy$ is path
438 independent. The statement was further exemplified using a fictitious example in Appendix C.

439 **Appendix C: A fictitious example to show how the LI method works**

440 ~~It is assumed that r~~Runoff (R , $10^{-3} \text{ m mm yr}^{-1}$) at a site ~~is assumed to increase~~ from 120 to 195 10^{-3}
441 m mm yr^{-1} with $\Delta R = 75 \text{ } 10^{-3} \text{ m mm yr}^{-1}$; meanwhile, precipitation (P , $10^{-3} \text{ m yr}^{-1} \text{ mm yr}^{-1}$) varies from
442 600 to 650 $10^{-3} \text{ m mm yr}^{-1}$ ($\Delta P = 75 \text{ } 10^{-3} \text{ m yr}^{-1} \text{ mm yr}^{-1}$) and the runoff coefficient (C_R , dimensionless)
443 ~~varies~~ from 0.2 to 0.3 ($\Delta C_R = 0.1$). The goal is to partition ΔR into the effects of the precipitation (ΔR_P)
444 and runoff coefficient (ΔR_{C_R}), provided that P and C_R are independent. We have a function $R = PC_R$ and
445 its partial derivatives $\partial R / \partial P = C_R$ and $\partial R / \partial C_R = P$. Given a path L along which P and C_R change and using
446 Eq. (3), the LI method evaluates ΔR_P and ΔR_{C_R} as:

$$447 \Delta R_{C_R} = \int_L \partial R / \partial C_R dC_R = \int_L P dC_R \text{ and } \Delta R_P = \int_L \partial R / \partial P dP = \int_L C_R dP \quad (C1)$$

设置了格式: 字体: Times New Roman

设置了格式: 字体: Times New Roman

域代码已更改

设置了格式: 字体: 倾斜

设置了格式: 字体: 倾斜

448 The result differs depending on L but the sum of ΔR_P and ΔR_{C_R} uniformly equals ΔR . This
 449 dynamic is ~~It will be~~ demonstrated using ~~Fig. 1(e)~~ Fig. 3, in which we considered that the x -axis
 450 represents C_R and the y -axis P . Point A denotes the initial state ($C_R = 0.2, P = 600$) and point C the
 451 terminal state ($C_R = 0.3, P = 650$). I calculated ΔR_P and ΔR_{C_R} along three fictitious paths as follows:

452 1) $L=AC$. Line segment AC has equation $P = 500C_R + 500, 0.2 \leq C_R \leq 0.3$. Let's take C_R as the
 453 parameter and write the equation in the parametric form as $P = 500C_R + 500, C_R = C_R, 0.2 \leq C_R \leq 0.3$. By
 454 substituting the equation into Eq. (C1), we have:

$$455 \quad \Delta R_{C_R} = \int_{AC} P dC_R = \int_{0.2}^{0.3} (500C_R + 500) dC_R = 62.5$$

$$456 \quad \Delta R_P = \int_{AC} C_R dP = \int_{AC} C_R d(500C_R + 500) = 500 \int_{0.2}^{0.3} C_R dC_R = 12.5$$

457 2) $L=AB+BC$. To evaluate on the broken line, we can evaluate separately on AB and BC and then sum
 458 them up. The equation for AB is $P = 600, 0.2 \leq C_R \leq 0.3$, ~~and while for BC is~~ $C_R = 0.3, 600 \leq P \leq 650$ ~~for~~
 459 ~~BC~~. Notes that a constant C_R or P implies that ~~$dC_R = 0$ or $dP = 0$~~ . Eq. (C1) then becomes:

$$460 \quad \Delta R_{C_R} = \int_{AB+BC} P dC_R = \int_{AB} P dC_R + \int_{BC} P dC_R = \int_{0.2}^{0.3} 600 dC_R + 0 = 60$$

$$461 \quad \Delta R_P = \int_{AB+BC} C_R dP = \int_{AB} C_R dP + \int_{BC} C_R dP = 0 + \int_{600}^{650} 0.3 dP = 15$$

462 3) $L=AD+DC$. The equation for AD is $C_R = 0.2, 600 \leq P \leq 650$ and is $P = 650, 0.2 \leq C_R \leq 0.3$ for DC.
 463 ΔR_P and ΔR_{C_R} are evaluated as:

$$464 \quad \Delta R_{C_R} = \int_{AD+DC} P dC_R = \int_{AD} P dC_R + \int_{DC} P dC_R = 0 + \int_{0.2}^{0.3} 650 dC_R = 65$$

$$465 \quad \Delta R_P = \int_{AD+DC} C_R dP = \int_{AD} C_R dP + \int_{DC} C_R dP = \int_{600}^{650} 0.2 dP + 0 = 10$$

466 As we expected, the sum of ΔR_P and ΔR_{C_R} persistently equals ΔR although ΔR_P and ΔR_{C_R} varies
 467 with L .

469 Appendix D: Mathematical proof of the path-averaged sensitivity Derivation of

$$470 \quad \Delta R = \overline{\lambda_P \Delta P} + \overline{\lambda_{C_R} \Delta C_R} + \overline{\lambda_n \Delta n}$$

471 If ~~we partition~~ the interval $[x_0, x_N]$ in ~~Fig. 1(e)~~ Fig. 3 is partitioned into N distinct bins of the same
 472 width $\Delta x_i = \Delta x/N$. Eq. (3a) can then be rewritten as:

$$473 \quad \Delta Z_x = \int_L f_x(x, y) dx = \lim_{\tau \rightarrow 0} \sum_{i=0}^{N-1} f_x(x_i, y_i) \Delta x_i = \lim_{\tau \rightarrow 0} N \Delta x_i \frac{\sum_{i=0}^{N-1} f_x(x_i, y_i)}{N} = \Delta x \lim_{\tau \rightarrow 0} \frac{\sum_{i=0}^{N-1} f_x(x_i, y_i)}{N} = \overline{\lambda_x} \Delta x$$

474 where $\overline{\lambda_x} = \lim_{\tau \rightarrow 0} \frac{\sum_{i=0}^{N-1} f_x(x_i, y_i)}{N}$, denoting the average of $f_x(x, y)$ along the curve L . Likewise, we have
 475 $\Delta Z_y = \overline{\lambda_y} \Delta y$, where $\overline{\lambda_y}$ denotes the average of $f_y(x, y)$ along the curve L . As a result, ~~we have~~:

$$\Delta Z = \bar{\lambda}_x \Delta x + \bar{\lambda}_y \Delta y \quad (D1)$$

The result can readily be extended to a function of three variables. Applying the mathematic derivation determined above to the MCY Equation-equation results in a precise form of Eq. (7):

$$\Delta R = \Delta R_P + \Delta R_{E_0} + \Delta R_n = \bar{\lambda}_P \Delta P + \bar{\lambda}_{E_0} \Delta E_0 + \bar{\lambda}_n \Delta n, \quad (D2)$$

where $\Delta R_P = \bar{\lambda}_P \Delta P$, $\Delta R_{E_0} = \bar{\lambda}_{E_0} \Delta E_0$, $\Delta R_n = \bar{\lambda}_n \Delta n$, and $\bar{\lambda}_P$, $\bar{\lambda}_{E_0}$ and $\bar{\lambda}_n$ denote the arithmetic mean of $\partial R / \partial P$, $\partial R / \partial E_0$, and $\partial R / \partial n$ along a path of climate and catchment changes, respectively. Because $\bar{\lambda}_P = \Delta R_P / \Delta P$, $\bar{\lambda}_{E_0} = \Delta R_{E_0} / \Delta E_0$, and $\bar{\lambda}_n = \Delta R_n / \Delta n$, $\bar{\lambda}_P$, $\bar{\lambda}_{E_0}$ and $\bar{\lambda}_n$ also implies-imply the runoff change due to a unit change in P , E_0 and n , respectively.

Appendix E: Path-averaged sensitivity in one-dimensional cases

Given a one-dimensional function $z=f(x)$ and its derivative $f'(x)$. We assumed that $f'(x)$ averages

$\bar{\lambda}_x$ over the range $(x, x + \Delta x)$, i.e., $\bar{\lambda}_x = \lim_{\tau \rightarrow 0} \frac{\sum_{i=1}^N f'(x_i)}{N}$. According to the mean value theorem for integrals,

$\bar{\lambda}_x = \int_x^{x+\Delta x} f'(x) dx / \Delta x$. In terms of the Newton-Leibniz formula, $\int_x^{x+\Delta x} f'(x) dx = f(x + \Delta x) - f(x) = \Delta z$.

Thus, we obtain: $\bar{\lambda}_x = \Delta z / \Delta x$.

Acknowledgments

This work was funded by the National Natural Science Foundation of China (41671278), the GDAS' Project of Science and Technology Development (2019GDASYL-0103043) and (2019GDASYL-0502004). I thank Mr. Y.Q. Zheng for his assistance with the mathematic derivations.

References

- Barnett, T. P., Pierce, D. W., Hidalgo, H. G., Bonfils, C., Santer, B. D., Das, T., Bala G., Woods, A. W., Nozawa, T., Mirin, A. A., Cayan D. R., and M. D. Dettinger: Human-induced changes in the hydrology of the western United States. *Science*, 319(5866), 1080-1083. <https://doi.org/10.1126/science.1152538>, 2008.
- Berghuijs, W. R., R. A. Woods: Correspondence: Space-time asymmetry undermines water yield assessment. *Nature Communications* 7, 11603. <https://doi.org/10.1038/ncomms11603>, 2016.
- Binley, A. M., Beven, K. J., Calver, A., and L. G. Watts: Changing responses in hydrology: assessing the uncertainty in physically based model predictions. *Water Resources Research*, 27(6), 1253-1261. <https://doi.org/10.1029/91WR00130>, 1991.
- Brown, A. E., Zhang, L., McMahon, T. A., Western, A. W. and R. A. Vertessy: A review of paired

设置了格式: 字体: (默认) Times New Roman, (中文) Times New Roman

设置了格式: 字体: Times New Roman, 倾斜

设置了格式: 字体: 倾斜

带格式的: 缩进: 首行缩进: 2.95 字符

域代码已更改

设置了格式: 字体: (中文) 宋体, 小四, 字体颜色: 黑色

域代码已更改

域代码已更改

设置了格式: 字体: 小四

域代码已更改

设置了格式: 字体: 倾斜

域代码已更改

域代码已更改

域代码已更改

设置了格式: 字体: 小四

设置了格式: 字体: 小四

设置了格式: 字体: 小四

域代码已更改

507 catchment studies for determining changes in water yield resulting from alterations in vegetation.
508 *Journal of Hydrology*, 310, 26–61. <https://doi.org/10.1016/j.jhydrol.2004.12.010>, 2005.

509 Budyko, M. I.: *Climate and Life*. Academic, N. Y. 1974.

510 Carmona, A. M., Sivapalan, M., Yaeger, M. A., and Poveda, G.: Regional patterns of interannual
511 variability of catchment water balances across the continental US: A Budyko framework. *Water*
512 *Resources Research*, 50, 9177–9193. <https://doi.org/10.1002/2014wr016013>, 2014.

513 Choudhury, B. J.: Evaluation of an empirical equation for annual evaporation using field observations
514 and results from a biophysical model. *Journal of Hydrology*, 216, 99–110.
515 [https://doi.org/10.1016/S0022-1694\(98\)00293-5](https://doi.org/10.1016/S0022-1694(98)00293-5), 1999.

516 Dey, P., and A. Mishra: Separating the impacts of climate change and human activities on streamflow: A
517 review of methodologies and critical assumptions. *Journal of Hydrology*, 548, 278-290.
518 <https://doi.org/10.1016/j.jhydrol.2017.03.014>, 2017.

519 Donohue, R. J., M. L. Roderick, and T. R. McVicar: On the importance of including vegetation dynamics
520 in Budyko 's hydrological model. *Hydrology and Earth System Sciences*, 11, 983 – 995.
521 <https://doi.org/10.5194/hess-11-983-2007>, 2007.

522 Gao, G., Ma, Y., and B. Fu: Multi-temporal scale changes of streamflow and sediment load in a loess
523 hilly watershed of China. *Hydrological Processes*, 30(3), 365-382, 10.1002/hyp.10585, 2016.

524 Gasser, T., M. Kechiar, P. Ciais, E. J. Burke, T. Kleinen, D. Zhu, Y. Huang, A. Ekici, and M. Obersteiner:
525 Path-dependent reductions in CO₂ emission budgets caused by permafrost carbon release. *Nature*
526 *Geoscience*, 11, 830–835. <https://doi.org/10.1038/s41561-018-0227-0>, 2018.

527 Jiang, C., Xiong, L., Wang, D., Liu, P., Guo, S., and Xu C.: Separating the impacts of climate change and
528 human activities on runoff using the Budyko-type equations with time-varying parameters. *Journal of*
529 *Hydrology*, 522, 326-338, 10.1016/j.jhydrol.2014.12.060, 2015.

530 Li, Z., Ning, T., Li, J., and D. Yang: Spatiotemporal variation in the attribution of streamflow changes
531 in a catchment on China's Loess Plateau. *Catena*, 158:1–8.
532 <https://doi.org/10.1016/j.catena.2017.06.008>, 2017.

533 Liang, W., D. Bai, F. Wang, B. Fu, J. Yan, S. Wang, Y. Yang, D. Long, and M. Feng: Quantifying the
534 impacts of climate change and ecological restoration on streamflow changes based on a Budyko
535 hydrological model in China's Loess Plateau. *Water Resources Research*, 51, 6500–6519.
536 <https://doi.org/10.1002/2014WR016589>, 2015.

537 Liu, J., Zhang, Q., Singh, V. P., and P. Shi: Contribution of multiple climatic variables and human
538 activities to streamflow changes across China. *Journal of Hydrology*, 545, 145-162.
539 <https://doi.org/10.1016/j.jhydrol.2016.12.016>, 2016.

540 Mezentsev, V. S.: More on the calculation of average total evaporation. *Meteorol. Gidrol.*, 5, 24–26, 1955.

541 Ning, T., Li, Z., and W. Liu: Vegetation dynamics and climate seasonality jointly control the
542 interannual catchment water balance in the Loess Plateau under the Budyko framework,
543 *Hydrology and Earth System Sciences*, 21, 1515-1526. <https://doi.org/10.5194/hess-2016-484>, 2017.

544 Roderick, M. L., and G. D. Farquhar: A simple framework for relating variations in runoff to variations
545 in climatic conditions and catchment properties. *Water Resources Research*, 47, W00G07,
546 <https://doi.org/10.1029/2010WR009826>, 2011.

547 Sankarasubramanian, A., R. M. Vogel, and J. F. Limbrunner: Climate elasticity of streamflow in the
548 United States. *Water Resources Research*, 37(6), 1771-1781. <https://doi.org/10.1029/2000WR900330>,

2001.

549
550 Schaake, J. C.: From climate to flow. *Climate Change and U.S. Water Resources*, edited by P. E.
551 Waggoner, chap. 8, pp. 177 - 206, John Wiley, N. Y. 1990.

552 Sivapalan, M., Yaeger, M. A., Harman, C. J., Xu, X. Y., and P. A. Troch: Functional model of water
553 balance variability at the catchment scale: 1. Evidence of hydrologic similarity and space-time
554 symmetry, *Water Resources Research*, 47, W02522, doi:10.1029/2010wr009568, 2011.

555 Sposito, G.: Understanding the Budyko equation. *Water*, 9(4), 236. <https://doi.org/10.3390/w9040236>,
556 2017.

557 Sun, Y., Tian, F., Yang, L., and H. Hu: Exploring the spatial variability of contributions from climate
558 variation and change in catchment properties to streamflow decrease in a mesoscale basin by three
559 different methods. *Journal of Hydrology*, 508(2), 170-180,
560 <https://doi.org/10.1016/j.jhydrol.2013.11.004>, 2014.

561 Wang, D., and M. Hejazi: Quantifying the relative contribution of the climate and direct human impacts
562 on mean annual streamflow in the contiguous United States. *Water Resources Research*, 47, W00J12,
563 <https://doi.org/10.1029/2010WR010283>, 2011.

564 Wang, W., Q. Shao, T. Yang, S. Peng, W. Xing, F. Sun, and Y. Luo: Quantitative assessment of the
565 impact of climate variability and human activities on runoff changes: A case study in four catchments
566 of the Haihe River basin, China. *Hydrological Processes*, 27(8), 1158–1174.
567 <https://doi.org/10.1002/hyp.9299>, 2013.

568 Wu, J., Miao, C., Wang, Y., Duan, Q., and X. Zhang: Contribution analysis of the long-term changes in
569 seasonal runoff on the Loess Plateau, China, using eight Budyko-based methods. *Journal of*
570 *hydrology*, 545, 263-275. <https://doi.org/10.1016/j.jhydrol.2016.12.050>, 2017a.

571 Wu, J., Miao, C., Zhang, X., Yang, T., and Q. Duan: Detecting the quantitative hydrological response to
572 changes in climate and human activities. *Science of the Total Environment*, 586, 328-337.
573 <https://doi.org/10.1016/j.scitotenv.2017.02.010>, 2017b.

574 Xu, X., Yang, D., Yang, H. and Lei, H.: Attribution analysis based on the Budyko hypothesis for detecting
575 the dominant cause of runoff decline in Haihe basin. *Journal of Hydrology*, 510: 530-540.
576 <http://dx.doi.org/10.1016/j.jhydrol.2013.12.052>, 2014.

577 Yang, H., D. Yang, Z. Lei, and F. Sun: New analytical derivation of the mean annual water-energy balance
578 equation. *Water Resources Research*, 44, W03410. <https://doi.org/10.1029/2007WR006135>, 2008.

579 Yang, H., and D. Yang: Derivation of climate elasticity of runoff to assess the effects of climate change
580 on annual runoff. *Water Resources Research*, 47, W07526. <https://doi.org/10.1029/2010WR009287>,
581 2011.

582 Yang, H., D. Yang, and Q. Hu: An error analysis of the Budyko hypothesis for assessing the contribution
583 of climate change to runoff. *Water Resources Research*, 50, 9620–9629. [https://doi.org/10.1002/](https://doi.org/10.1002/2014WR015451)
584 [2014WR015451](https://doi.org/10.1002/2014WR015451), 2014.

585 Zhao, Q. L., Liu, X. L., Ditmar, P., Siemes, C., Revtova, E., Hashemi-Farahani, H., and R. Klees: Water
586 storage variations of the Yangtze, Yellow, and Zhujiang river basins derived from the DEOS Mass
587 Transport (DMT-1) model. *Science China-Earth Sciences*, 54, 667-677.
588 <https://doi.org/10.1007/s11430-010-4096-7>, 2011.

589 Zhang, S., H. Yang, D. Yang, and A. W. Jayawardena: Quantifying the effect of vegetation change on the
590 regional water balance within the Budyko framework. *Geophysical Research Letters*, 43, 1140–1148.

591 <https://doi.org/10.1002/2015GL066952>, 2016.

592 Zhang, L., Dawes, W. R. and G. R. Walker: Response of mean annual evapotranspiration to vegetation
 593 changes at catchment scale. *Water Resources Research* 37, 701–708. doi; 10.1029/2000WR900325,
 594 2001.

595 Zhang, L., F. Zhao, A. Brown, Y. Chen, A. Davidson, and R. Dixon: Estimating Impact of Plantation
 596 Expansions on Streamflow Regime and Water Allocation. CSIRO Water for a Healthy Country,
 597 Canberra, Australia. 2010.

598 Zhang, L., F. Zhao, Y. Chen, and R. N. M. Dixon: Estimating effects of plantation expansion and climate
 599 variability on streamflow for catchments in Australia. *Water Resources Research*, 47, W12539,
 600 <https://doi.org/10.1029/2011WR010711>, 2011.

601 Zheng, H., L. Zhang, R. Zhu, C. Liu, Y. Sato, and Y. Fukushima: Responses of streamflow to climate and
 602 land surface change in the headwaters of the Yellow River Basin. *Water Resources Research*, 45,
 603 W00A19. <https://doi.org/10.1029/2007WR006665>, 2009.

604 Zhou, S., B. Yu, L. Zhang, Y. Huang, M. Pan, and G. Wang (2016), A new method to partition climate
 605 and catchment effect on the mean annual runoff based on the Budyko complementary relationship.
 606 *Water Resources Research*, 52, 7163–7177. <https://doi.org/10.1002/2016WR019046>, 2016.

632 **Table 1.** Summary of the long-term hydrometeorological characteristics of the selected catchments^a

Catchment No. ^b	Area (10 ³ km ²)	<i>R</i>	<i>P</i>	<i>E</i> ₀	<i>n</i>	<i>AI</i>	Reference Period	Evaluation Period	The Last final Subperiod
1	391	218	1014	935	3.5	0.92	1933-1955	1956-2008	1998-2008
2	16.64	32.9	634	1087	3.16	1.71	1979-1984	1985-2008	1999-2008

设置了格式: 字体: 10 磅

设置了格式: 字体: 10 磅, 上标

3	559	183	787	780	2.68	0.99	1960-1978	1979-2000	1993-2000
4	606	73	729	998	3.07	1.37	1971-1995	1996-2009	2003-2009
5	760	77.9	689	997	2.66	1.45	1970-1995	1996-2009	2003-2009
6	502	57.2	730	988	3.59	1.35	1974-1995	1996-2008	1996-2008
7	673	431	1013	953	1.34	0.94	1947-1955	1956-2008	1998-2008
8	390	139	840	1021	2.61	1.22	1966-1980	1981-2005	1995-2005
9	1130	20.7	633	1077	3.79	1.7	1972-1982	1983-2007	1997-2007
10	3.2	37.5	631	954	3.49	1.51	1989-1991	1992-2009	1999-2009
11	1.95	111	767	901	3.06	1.18	1990-1992	1993-2005	1993-2005
12	89	272	963	826	2.82	0.86	1958-1965	1966-1999	1987-1999
13	243	38.5	735	1010	4.27	1.37	1989-1995	1996-2007	1996-2007
14	56.35	65.8	744	1007	3.35	1.35	1989-1995	1996-2008	1996-2008
15	14484	385	893	1022	1.11	1.14	1970-1989	1990-2000	1990-2000
16	38625	461	985	1087	1.03	1.1	1970-1989	1990-2000	1990-2000
17	59115	388	897	1161	1.02	1.29	1970-1989	1990-2000	1990-2000
18	95217	371	881	1169	1.03	1.33	1970-1989	1990-2000	1990-2000
19	121,972	171	507	768	1.17	1.52	1960-1990	1991-2000	1991-2000
20	106,500	60.5	535	905	2.25	1.69	1960-1970	1971-2009	1999-2009
21	5891	34.4	506	964	2.54	1.91	1952-1996	1997-2011	2004-2011

^a R , P , and E_0 represents the mean annual runoff, precipitation and potential evaporation, all in 10^3 m mm yr^{-1} . n (dimensionless) is the parameter representing catchment properties in the MCY equation. AI is the dimensionless aridity index ($AI = E_0/P$). Data of Catchments 1-14 were derived from Zhang *et al.* (2010). Data of Catchments 15-18 were from Sun *et al.* (2014). Data of Catchments 19-21 were from Zheng *et al.* (2009), Jiang *et al.* (2015), and Gao *et al.* (2016), respectively. I used the change points given in the literatures to divide the observation period into the reference and elevation periods. The LI method further divides the evaluation period into a number of subperiods. The column “The ~~Last final~~ Subperiod” denotes the ~~last final onesubperiod, which, which~~ was used as the evaluation period for the total differential method, the decomposition method and the complementary method. The bold and italic rows denote that the column “Evaluation Period” is the same as the column “The ~~Last final~~ Subperiod”.

^bCatchments 1-14 are in Australia and the others are in China. 1: Adjungbilly CK; 2: Batalling Ck; 3: Bombala River; 4: Crawford River; 5: Darlot Ck; 6: Eumeralla River; 7: Goobarragandra CK; 8: Jingellic CK; 9: Mosquito CK; 10: Pine Ck; 11: Red Hill; 12: Traralgon Ck; 13: Upper Denmark River; 14: Yate Flat Ck; 15: Yangxian station, Hang River; 16: Ankang station, Hang River; 17: Baihe station, Hang River; 18: Danjiangkou station, Hang River; 19: Headwaters of the Yellow River Basin; 20: Wei River; 21: Yan River.

656
657

Table 2. Comparisons of R (mm yr⁻¹), P (mm yr⁻¹), E_0 (mm yr⁻¹), and n (dimensionless) between the reference and the evaluation periods^a

Catchment No.	R_1	R_2	P_1	P_2	E_{01}	E_{02}	n_1	n_2	ΔR	ΔP	ΔE_0	Δn
1	223	216	959	1038	950	928	2.7	4.1	-7.2	79.2	-21	1.4
2	40.6	31	655	629	1087	1087	3	3.2	-9.7	-27	0	0.2
3	249	127	847	736	780	780	2.3	3.2	-122	-112	0.4	0.9
4	90.6	41.5	753	685	1002	989	2.9	3.7	-49	-67	-13	0.8
5	94.9	46.3	718	633	1000	992	2.5	3	-49	-85	-9	0.5
6	70.8	34.3	756	687	989	987	3.4	4.1	-36	-69	-2	0.6
7	575	406	1123	995	931	957	1.1	1.4	-169	-128	25	0.3
8	139	139	871	821	1043	1008	2.7	2.5	-0.4	-50	-35	0
9	24.1	19.2	659	621	1100	1067	3.7	3.8	-4.9	-37	-33	0.1
10	116	24.3	588	638	927	958	1.7	4.2	-92	50.4	31	2.5
11	297	68	986	716	884	905	2.3	3.6	-229	-271	22	1.3
12	301	265	992	956	820	828	2.7	2.8	-36	-36	7.4	0.1
13	48.5	32.6	752	725	991	1021	4.2	4.4	-16	-28	30	0.2
14	90.4	52.6	753	739	991	1015	2.9	3.7	-38	-14	24	0.8
15	435	295	948	795	1008	1047	1.1	1.2	-139	-153	38	0.1
16	520	353	1035	894	1074	1109	1	1.2	-167	-141	35	0.2
17	441	291	939	820	1149	1182	1	1.2	-151	-119	33	0.2
18	412	296	913	821	1163	1179	1	1.1	-116	-92	15	0.2
19	180	144	512	491	774	751	1.1	1.3	-36	-21	-23	0.2
20	90.2	52.1	585	520	895	908	2.1	2.3	-38	-65	13	0.2
21	37.7	24.6	521	462	954	995	2.6	2.5	-13	-59	41	0

658 ^aThe subscript "1" denotes the reference period and "2" denotes the evaluation period. $\Delta X = X_2 - X_1$ (X as a
659 substitute for R , P , E_0 , and n).
660

661
662
663
664
665
666
667
668
669
670
671
672
673
674
675
676

677 **Table 3.** Effects of precipitation (ΔR_P , 10^{-3} mm yr⁻¹), potential evapotranspiration (ΔR_{E_0} , 10^{-3} mm
678 yr⁻¹), and catchment- changes (ΔR_n , 10^{-3} mm yr⁻¹) on the mean annual runoff resulting determined from
679 the four evaluated methods

Catchment NO. ^a	LI Method			Decomposition Method	Total Differential Method			Complementary Method		
	ΔR_P	ΔR_{E_0}	ΔR_n	ΔR_n	ΔR_P	ΔR_{E_0}	ΔR_n	ΔR_P	ΔR_{E_0}	ΔR_n
1	-70.9	-8.99	-24.3	-44.6	-67	4.82	-62	-60.7	4.34	-47.3
2	-6.49	0.95	-9.74	-9.65	-7.2	1.3	-13	-6.23	1.13	-10.2
3	-89	25.9	-140	-128	-104	26.6	-483	-88	25.7	-140
4	-18.1	2.09	-35.4	-36.3	-18	2.37	-58	-14.8	1.99	-38.5
5	-27.9	1.14	-21.3	-18.6	-34	1.18	-27	-28.1	0.97	-20.9
6	-19.9	0.29	-16.7	-14.9	-24	0.36	-22	-19.9	0.29	-16.7
7	-211	-7.19	-101	-90.9	-236	-6.9	-134	-211	-6.21	-102
8	-32.2	12.3	-14.4	-12.6	-35	12.6	-15	-32.9	11.9	-13.3
9	-11.8	3.02	-9.96	-8.45	-13	0.85	-20	-8.76	0.56	-10.5
10	19.47	-5.61	-119	-96.5	0.91	-10	-291	0.56	-6.53	-99.1
11	-150	-7.46	-71.8	-60.7	-188	-9.4	-113	-144	-7.04	-78.3
12	-9.88	-3.99	-79.2	-82	-11	-0.5	-154	-10.8	-0.57	-81.6
13	-6.98	-4.36	-4.54	-4.21	-8	-5.1	-5.2	-7	-4.38	-4.51
14	-4.84	-4.42	-28.7	-27.9	-5.6	-5	-37	-4.85	-4.4	-28.6
15	-104	-8.56	-24.8	-23	-110	-9.4	-27	-103	-8.52	-25.1
16	-99.3	-7.99	-58.8	-56	-105	-8.3	-68	-99	-7.92	-59.1
17	-78.8	-6.26	-63.9	-61	-84	-6.5	-76	-78.6	-6.2	-64.2
18	-60.1	-2.79	-53.5	-52	-64	-2.9	-62	-60	-2.77	-53.6
19	-11.9	3.89	-27.6	-27	-12	3.81	-31	-11.9	3.85	-27.5
20	-27.5	-2.46	-18.5	-17	-31	-4.4	-26	-25.5	-3.47	-19.5
21	-10.4	-3.47	-2.11	-3.4	-9.9	-4.8	-4.8	-8.27	-3.86	-3.82

680 ^aThe bold and italic numbers denote that the evaluation period comprises a single subperiod.
681
682
683
684
685
686
687
688
689
690
691
692
693

设置了格式: 字体: 非加粗
域代码已更改
域代码已更改

694
695

Table 4. Comparisons of the path-averaged sensitivities with the point sensitivities of runoff^{a, b}

Catchment NO.	$\bar{\lambda}_P$	$\bar{\lambda}_{E_0}$	$\bar{\lambda}_n$	λ_{Pf}	λ_{E_0f}	λ_{nf}
1	0.68	-0.55	-17	0.621	-0.39	-71.8
2	0.2	-0.08	-27.3	0.227	-0.1	-30.9
3	0.58	-0.36	-26.7	0.68	-0.42	-79
4	0.3	-0.16	-30.5	0.39	-0.2	-50.1
5	0.33	-0.14	-43.1	0.394	-0.19	-59.4
6	0.29	-0.16	-26.5	0.352	-0.2	-34.9
7	0.71	-0.32	-223	0.781	-0.33	-299
8	0.49	-0.26	-77.9	0.478	-0.27	-64.9
9	0.16	-0.07	-11.8	0.161	-0.07	-17.6
10	0.27	-0.12	-40.9	0.45	-0.16	-99.9
11	0.55	-0.35	-56.1	0.695	-0.44	-88.2
12	0.72	-0.45	-57.3	0.74	-0.53	-61.1
13	0.25	-0.15	-19.8	0.29	-0.17	-22.5
14	0.34	-0.18	-37.2	0.393	-0.21	-48.6
15	0.68	-0.22	-275	0.719	-0.25	-303
16	0.7	-0.23	-326	0.745	-0.24	-378
17	0.66	-0.19	-320	0.708	-0.2	-378
18	0.65	-0.19	-315	0.692	-0.19	-363
19	0.58	-0.17	-153	0.602	-0.17	-175
20	0.32	-0.12	-50.1	0.402	-0.16	-69.6
21	0.2	-0.06	-29.2	0.234	-0.09	-34

带格式表格

696
697

^a $\bar{\lambda}_P$ (10^{-3}mm^{-1}), $\bar{\lambda}_{E_0}$ ($10^{-3} \text{m}^{-1} \text{mm}^{-1}$), and $\bar{\lambda}_n$ (dimensionless) represent the path-averaged sensitivities of runoff to precipitation, potential evaporation, and catchment properties (see Appendix D). If the evaluation period comprises only one subperiod, $\bar{\lambda}_P$, $\bar{\lambda}_{E_0}$ and $\bar{\lambda}_n$ was calculated as: $\bar{\lambda}_P = \Delta R_P / \Delta P$, $\bar{\lambda}_{E_0} = \Delta R_{E_0} / \Delta E_0$, and $\bar{\lambda}_n = \Delta R_n / \Delta n$. If the evaluation period

698
699

comprises $N > 1$ subperiods, the equations become:

700
701

$\bar{\lambda}_P = \sum_{i=1}^N |\Delta R_{Pi}| / \sum_{i=1}^N |\Delta P_i|$, $\bar{\lambda}_{E_0} = -\sum_{i=1}^N |\Delta R_{E_0i}| / \sum_{i=1}^N |\Delta E_{0i}|$, and

702
703

$\bar{\lambda}_n = -\sum_{i=1}^N |\Delta R_{ni}| / \sum_{i=1}^N |\Delta n_i|$, where the subscript i denotes the i th subperiod.

704
705

^b λ_P , λ_{E_0} , and λ_n represent the point sensitivities of runoff of the total differential method. The subscript "f" represents a forward approximation, i.e. which was calculated by substituting the observed mean annual values of the reference period into Eq. (2) to calculate the sensitivities, while the subscript "b" represents a backward approximation, i.e. substituting the observed mean annual values of the evaluation period into Eq. (2).

设置了格式: 字体: 非加粗

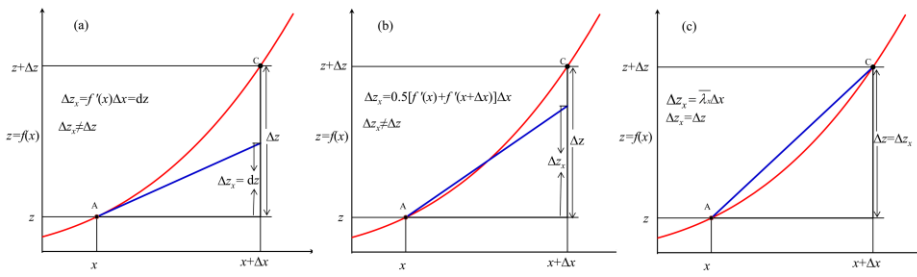
设置了格式: 字体: (中文) Calibri, 非加粗

设置了格式: 字体: 倾斜

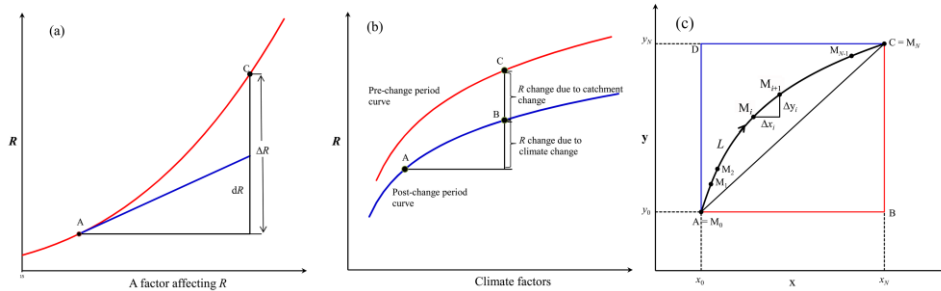
设置了格式: 字体: 倾斜

706
707

708
709



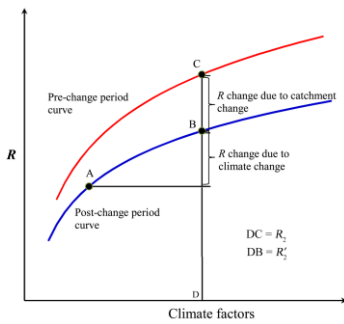
710
711
712



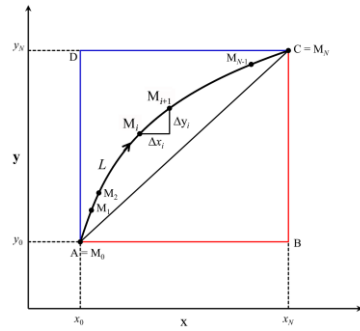
713
714
715
716
717
718
719

Fig. 41. For a non-linear function $z=f(x)$, the total differential method (a) and the complementary method (b) fails to accurately estimate the effect (Δz_x) of x on z when x changes by Δx , but the LI method (c) does. For a univariate function, the z change is exclusively driven by x , so that Δz_x should be equal to Δz . $\Delta z_x = \Delta z$ in (c) but not in (a) and (b). $\bar{\lambda}_x$ in (c) represents the average sensitivity along the curve AC and $\bar{\lambda}_x = \Delta z / \Delta x$, see Appendix E for details.

- 域代码已更改
- 域代码已更改
- 设置了格式: 字体: 倾斜
- 设置了格式: 字体: 倾斜
- 域代码已更改
- 域代码已更改
- 域代码已更改
- 域代码已更改
- 域代码已更改
- 域代码已更改



720
721 **Fig. 2.** A schematic plot to illustrate the decomposition method. Point A denotes the initial state (the
722 reference) and Point C denotes the terminal state (the evaluation period). R_2 represents the mean annual
723 runoff of the evaluation period, and R_1^c the mean annual runoff given the climate conditions of the
724 evaluation period and the catchment conditions of the reference period. See Section 2.4 for details.
725
726



727
728 **Fig. 3.** A schematic plot illustrating the LI method.

729 A schematic plot to illustrate (a) the total differential method, (b) the decomposition method, and (c) the
730 LI method. Point A denotes the initial state and Point C the terminal state. Notes that unlike (a) and (b),
731 the y axis is not R in (c).
732
733

域代码已更改

设置了格式: 字体: 10 磅, 加粗

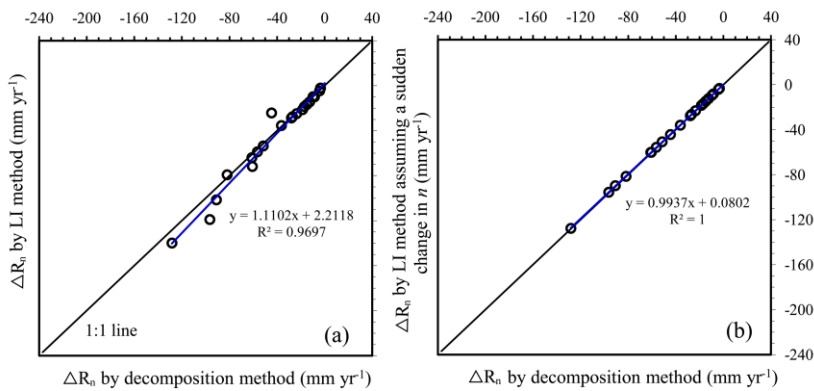
带格式的: 正文, 左

带格式的: 正文, 左

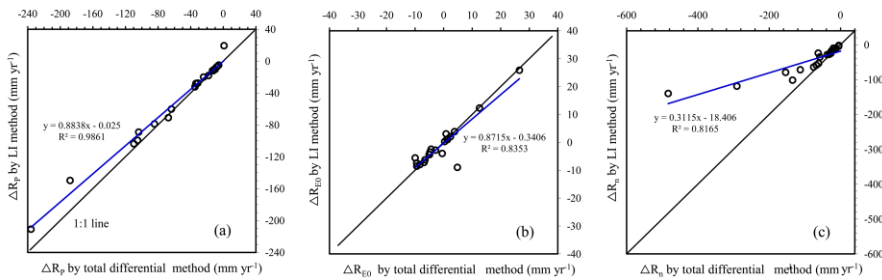
设置了格式: 字体: 10 磅, 加粗

设置了格式: 字体: 10 磅, 加粗

带格式的: 正文, 左



734 **Fig. 4.** Comparisons between the LI method and the decomposition method. (a) Comparison of the
 735 estimated contributions to the runoff changes from the catchment changes ($\Delta R_n - \Delta R_T$); (b) the
 736 decomposition method is equivalent to the LI method that assumes a sudden change in catchment
 737 properties following climate change. In this case, the integral path of the LI method is-can be considered
 738 as the broken line AB+BC in Fig. 4(e) Fig. 3 (x represents climate factors and y catchment properties, i.e.
 739 n) and $\Delta R_n = \int_{AB+BC} \frac{\partial R}{\partial n} dn = \int_{AB} \frac{\partial R}{\partial n} dn + \int_{BC} \frac{\partial R}{\partial n} dn = 0 + \int_{BC} \frac{\partial R}{\partial n} dn = \int_{n_1}^{n_2} f_n(P_2, E_{o2}, n) dn$, where the subscript "1"
 740 denotes the reference period and "2" denotes the last final subperiod of the evaluation period.



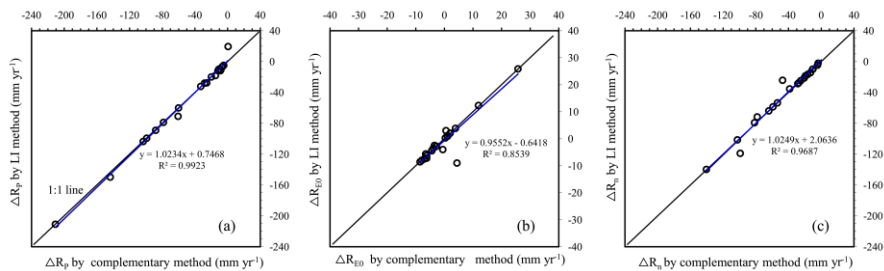
744 **Fig. 5.** Comparisons of the estimated contribution to runoff from the changes in (a) precipitation
 745 ($\Delta R_P - \Delta R_T$), (b) potential evapotranspiration ($\Delta R_{E_o} - \Delta R_T$), and (c) catchment properties ($\Delta R_n - \Delta R_T$) between
 746 the LI method and the total differential method.

域代码已更改

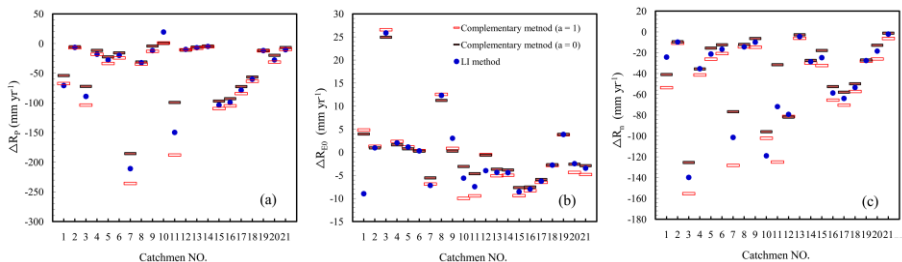
域代码已更改

域代码已更改

域代码已更改



749 **Fig. 4** Fig. 6. Comparisons of (a) ΔR_P , (b) ΔR_{E_0} , and (c) ΔR_n between the LI method and the
 750 complementary method ($a = 0.5$).
 751
 752



753 **Fig. 5** Fig. 7. Comparisons of (a) ΔR_P , (b) ΔR_{E_0} , and (c) ΔR_n by the LI
 754 method with the upper ($a=1$) and lower ($a=0$) bounds given by the complementary method. According to
 755 Zhou *et al.* (2016), ΔR_P , ΔR_{E_0} , and ΔR_n reach their the upper and lower bounds of ΔR_P , ΔR_{E_0} , and ΔR_n
 756 are reached when a is 0 or 1.
 757
 758
 759
 760
 761

域代码已更改
 域代码已更改
 域代码已更改

域代码已更改
 域代码已更改
 域代码已更改
 域代码已更改
 域代码已更改
 域代码已更改

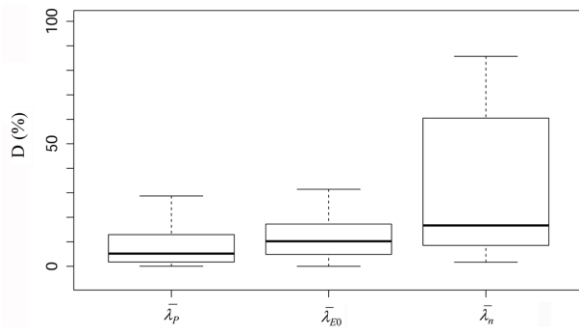


Fig. 8. Boxplots showing the temporal variability of the path-averaged sensitivities of water yield to precipitation ($\bar{\lambda}_P$), potential evapotranspiration ($\bar{\lambda}_{E0}$), and catchment properties ($\bar{\lambda}_n$). D (%) was calculated as the relative difference between the sensitivity of the whole evaluation period and that of a subperiod. In the calculations, I excluded the catchments ~~that had a whose~~ evaluation periods ~~were not long enough to comprise~~ only one two or more subperiods. ~~The Box-boxes~~ spans the inter-quartile range (IQR) and ~~the~~ solid lines are medians. ~~The W~~whiskers represent ~~the~~ data range, excluding statistical outliers, which extend more than 1.5IQR from the box ends.

762
763
764
765
766
767
768
769
770
771
772
773
774
775
776
777
778
779
780
781
782
783
784
785
786
787
788
789
790
791
792
793
794
795

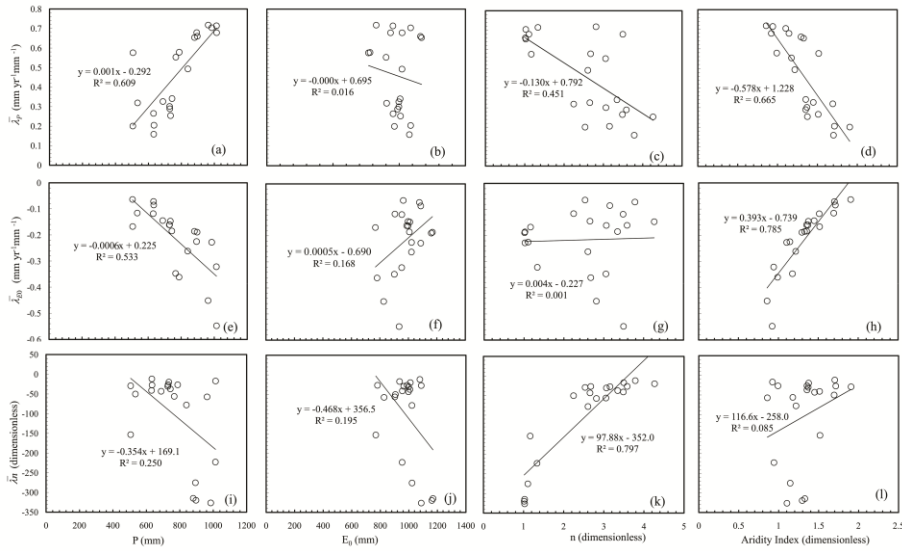


Fig. 7 Fig. 9. $\bar{\lambda}_P$, $\bar{\lambda}_{E0}$ and $\bar{\lambda}_n$ in correlation with P , E_0 , n , and aridity index.

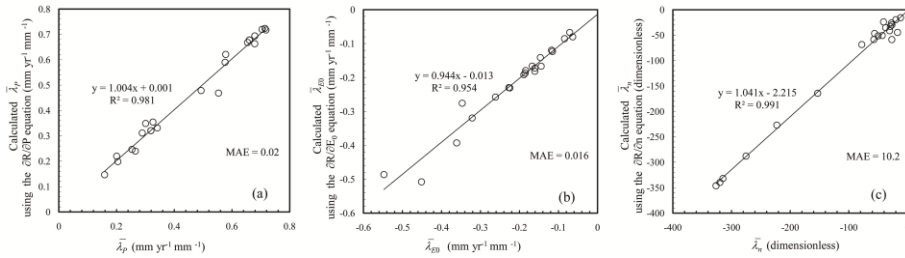
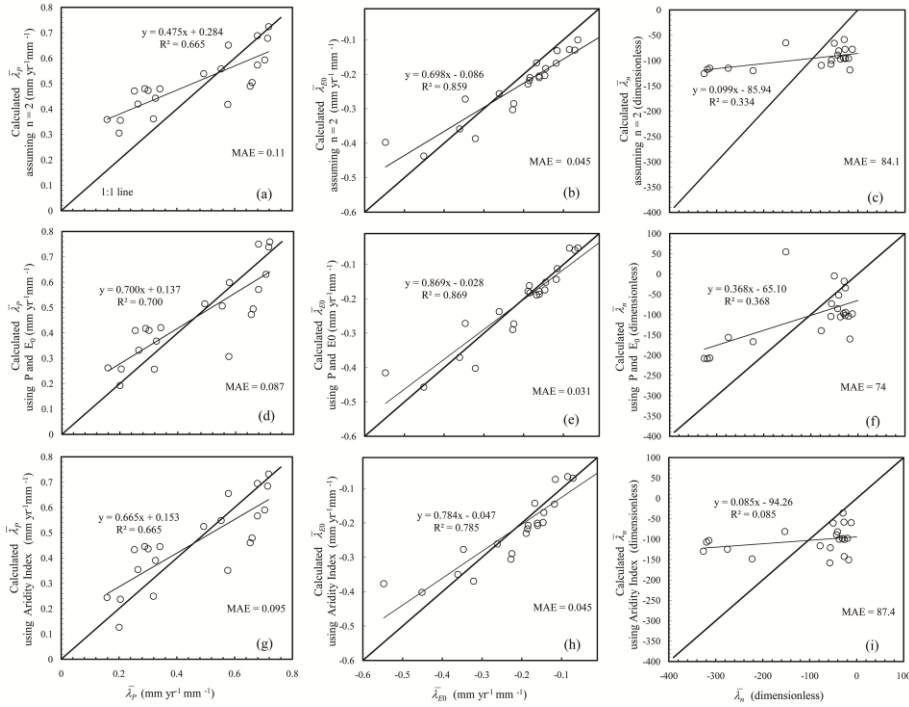


Fig. 8 Fig. 10. Comparisons of $\bar{\lambda}_P$, $\bar{\lambda}_{E0}$ and $\bar{\lambda}_n$ (given in Table 4) with those predicted using Eq. (2) with the long-term mean values of P , E_0 , and n as inputs. $MAE = N^{-1} \sum_{i=1}^N |O_i - P_i|$, is the mean absolute error, where O and P are values that actually encountered (given in Table 4) and predicted using Eq. (2) respectively, and N is the number of selected catchments.



810

811

812

813

814

815

816

817

Fig. 11. Comparisons of $\overline{\lambda_P}$, $\overline{\lambda_{E0}}$ and $\overline{\lambda_n}$ with those predicted by the three strategies. (a)-(c) **Predicted** by Eq. (2) with a constant n ($n = 2$), (d)-(f) **predicted** by the regression equations established using P and E_0 : $\overline{\lambda_P} = 0.0011P - 0.0006E_0 + 0.21$ ($R^2=0.7$), $\overline{\lambda_{E0}} = 0.0007P - 0.0007E_0 - 0.38$ ($R^2=0.87$), and $\overline{\lambda_n} = -0.302P - 0.372E_0 + 493$ ($R^2=0.37$), and (g)-(i) **predicted** by the regression equations established using only the aridity index, as shown in Fig. 9 (d), (h) and (i). MAE was calculated **using the same procedure as for in Fig. 8 Fig. 10.**

818

819

820

带格式的: 左, 孤行控制